Electronic Supplementary Material (ESI) for CrystEngComm.

Crystallisation of organic hydrates by sublimation

Alexandra L. Volkwyn and Delia A. Haynes

Department of Chemistry and Polymer Science, Stellenbosch University, P. Bag X1, Matieland, 7602, Stellenbosch, Republic of South Africa. Email: dhaynes@sun.ac.za

Electronic Supplementary Information

Contents

CSD refcodes

The relevant CSD refcodes for the compounds used in this study are given in Tables S1-S5 below.

1 oxalic acid (OA)
2 isonicotinamide (INAM)
3 theophylline (THE)
4 caffeine (CAF)
5 1,4-diazabicyclo[2.2.2]octane (DABCO)

Table S1. Different polymorphic forms of dihydrate and anhydrous forms of OA, with corresponding CSD refcodes and labelling.

OA

Anhydrous polymorphs		Dihydrate polymorphs	
CSD refcode	**Compound label**	**CSD refcode**	**Compound label**
OXALAC06[1] (α polymorph)	**1A-a**	OXACDH11[3]	**1H-a**
OXALAC07[2] (β polymorph)	**1A-b**		

Table S2. Different polymorphic forms of monohydrate and anhydrous forms of INAM, with corresponding CSD refcodes and labelling.

INAM

Anhydrous polymorphs		Monohydrate polymorphs	
CSD refcode	**Compound label**	**CSD refcode**	**Compound label**
EHOWIH[4]	**2A-a**	MOVTIB01[6]	**2H-a**
EHOWIH02[4]	**2A-b**	MOVTIB02[6]	**2H-b**
EHOWIH05[5]	**2A-c**		

Table S3. Different polymorphic forms of monohydrate and anhydrous forms of THE, with corresponding CSD refcodes and labelling.

THE

Anhydrous polymorphs		Monohydrate polymorphs	
CSD refcode	**Compound label**	**CSD refcode**	**Compound label**
BAPLOT01[7]	**3A-a**	THEOPH05[10]	**3H-a**
BAPLOT02[8]	**3A-b**		
BAPLOT05[9]	**3A-c**		

Table S4. Different polymorphic forms of monohydrate and anhydrous forms of CAF, with corresponding CSD refcodes and labelling.

CAF

Anhydrous polymorphs		Monohydrate polymorphs	
CSD refcode	**Compound label**	**CSD refcode**	**Compound label**
NIWFEE04[11] (α polymorph)	**4A-a**	CAFINE[12]	**4H-a**
NIWFEE05[11] (β polymorph)	**4A-b**		

Table S5. Different polymorphic forms of mono/hexa -hydrate and anhydrous forms of DABCO, with corresponding CSD refcodes and labelling.

DABCO

Anhydrous polymorphs		Hydrate polymorphs	
CSD refcode	**Compound label**	**CSD refcode**	**Compound label**
TETDAM05[13]	**5A-a**	Monohydrate (form I) QOHYAO[14]	**5H-a**
		Monohydrate (form II) QOHYAO01[15]	**5H-b**
		Hexahydrate QOHYES[14]	**5H-c**

Characterisation of materials

Materials as purchased

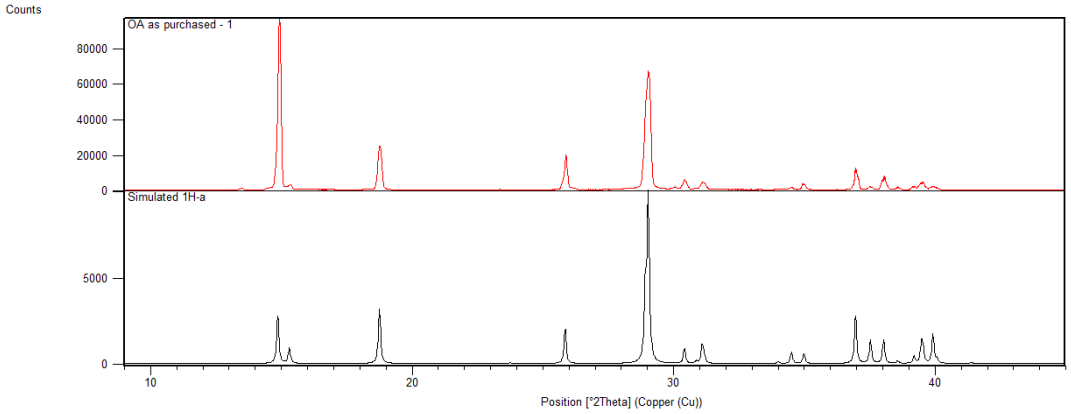

Figure S1. PXRD pattern of **1** as purchased (red) compared to simulated powder pattern of **1H-a** (black).

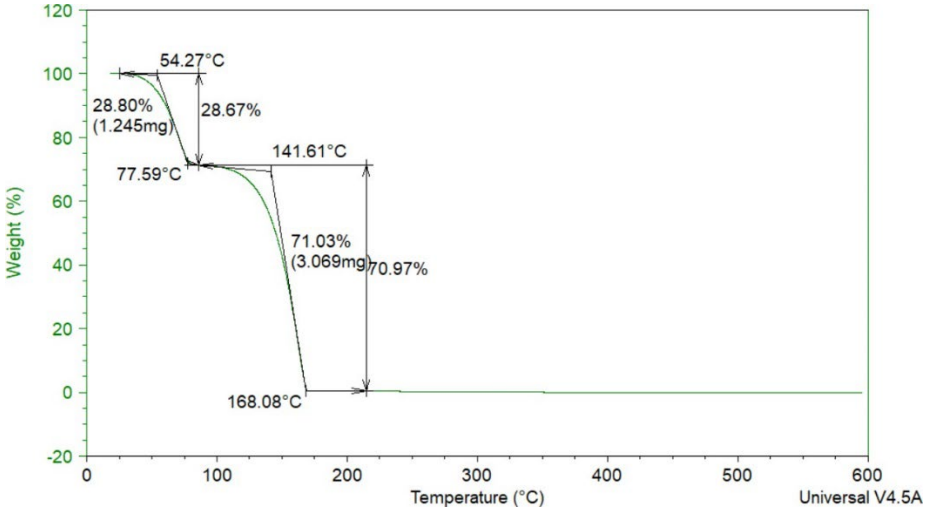

Figure S2. TGA curve of **1** as purchased with a mass loss of 28.67% water (calculated mass loss for two waters 28.58%).

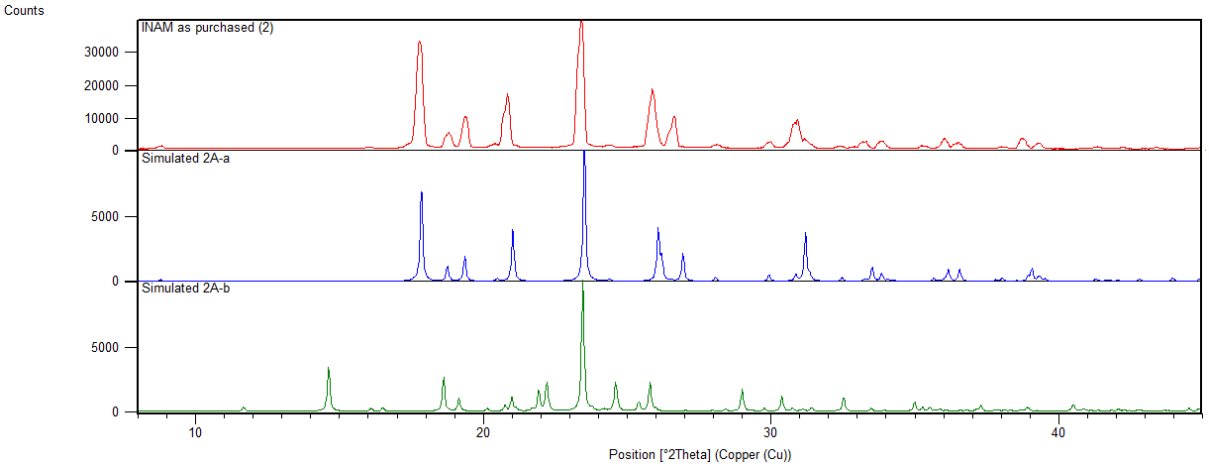

Figure S3. PXRD pattern of **2** as purchased (red) compared to simulated powder pattern of **2A-a** (blue) and **2A-b** (green).

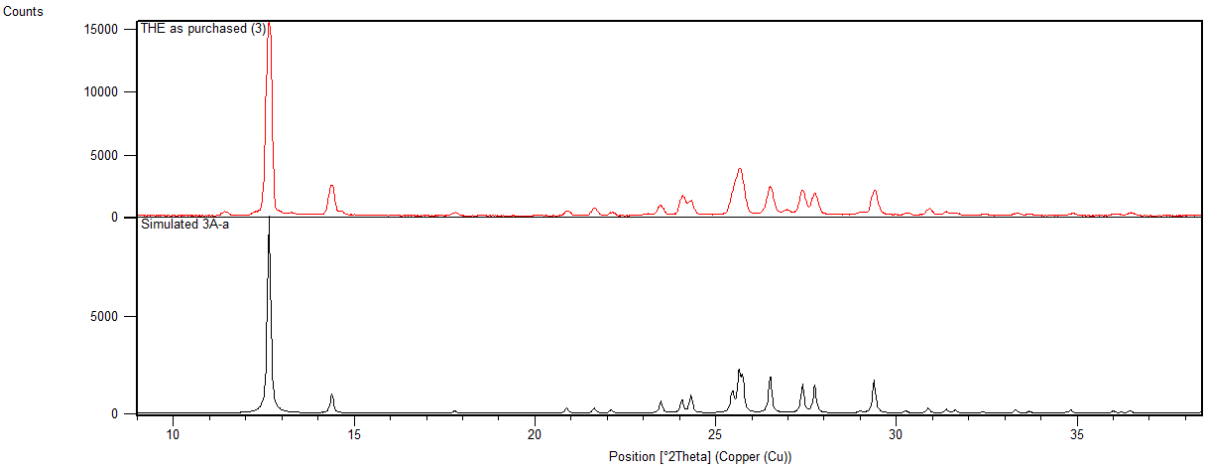

Figure S4. PXRD pattern of **3** as purchased (red) compared to simulated powder pattern of **3A-a** (black).

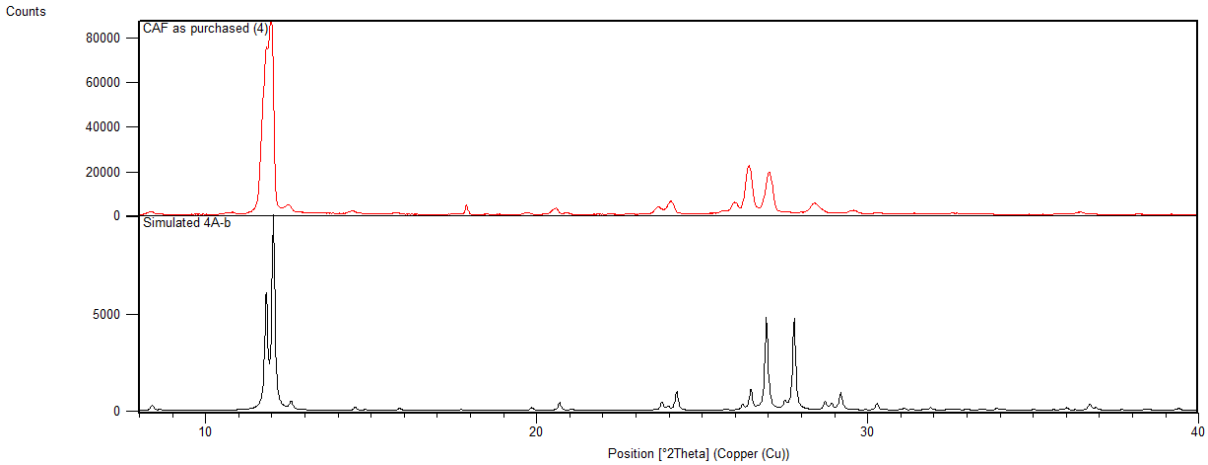

Figure S5. PXRD pattern of **4** as purchased (red) compared to simulated powder pattern of **4A-b** (black).

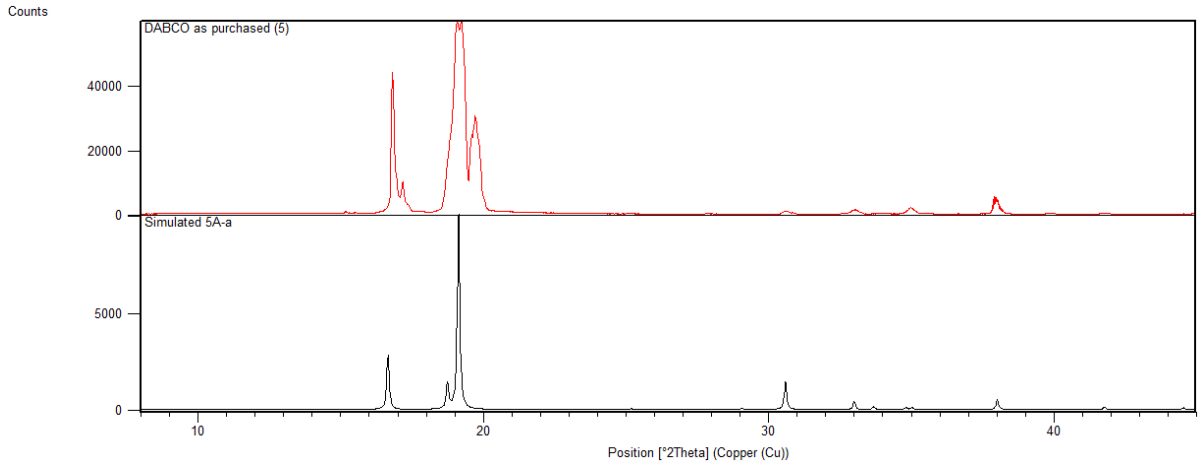

Figure S6. PXRD pattern of **5** as purchased (red) compared to simulated powder pattern of **5A-a** (black).

Synthesised materials

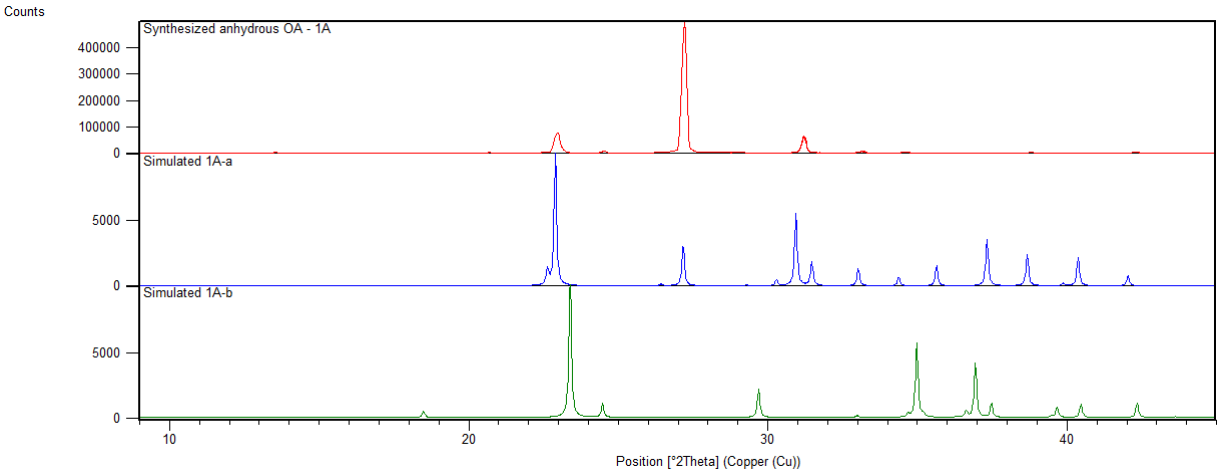

Figure S7. PXRD pattern of synthesised anhydrous OA **1A** (red) compared to simulated powder patterns.

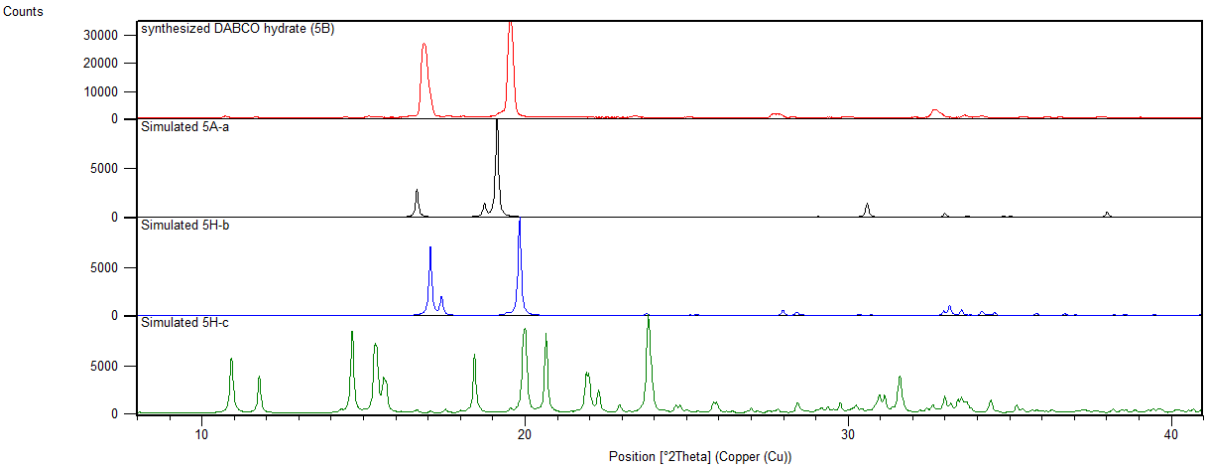

Figure S8. PXRD pattern of synthesised DABCO hydrate **5B** (red) compared to simulated powder patterns of the known hydrate forms.

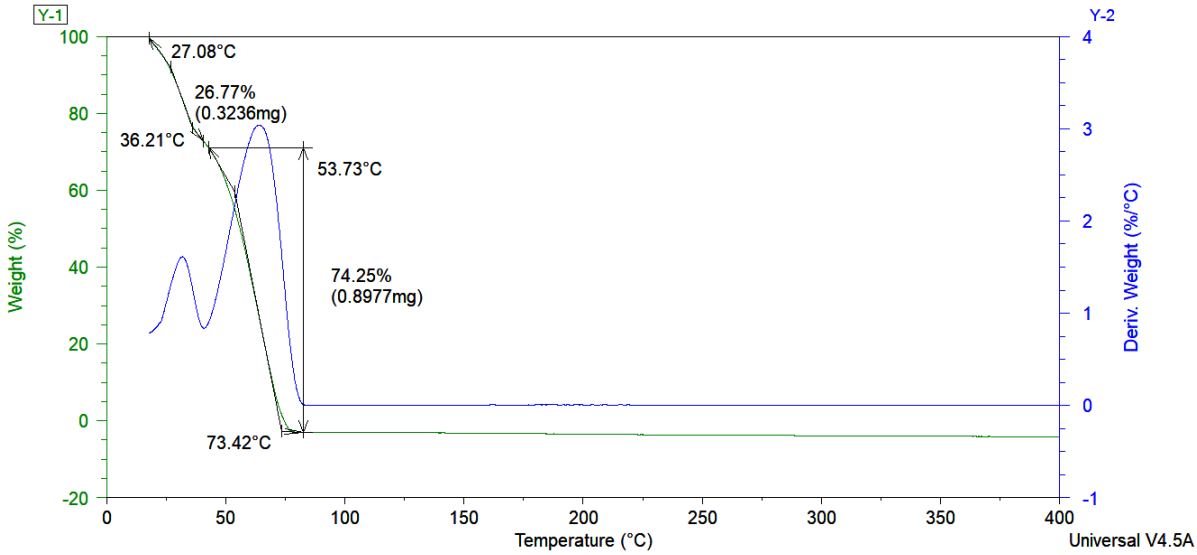

Figure S9. TGA of synthesised DABCO hydrate (**5B**) with a mass loss of 26.77% water (expected calculated mass loss of 13.84% water for DABCO monohydrate and 49.07% for DABCO hexahydrate).

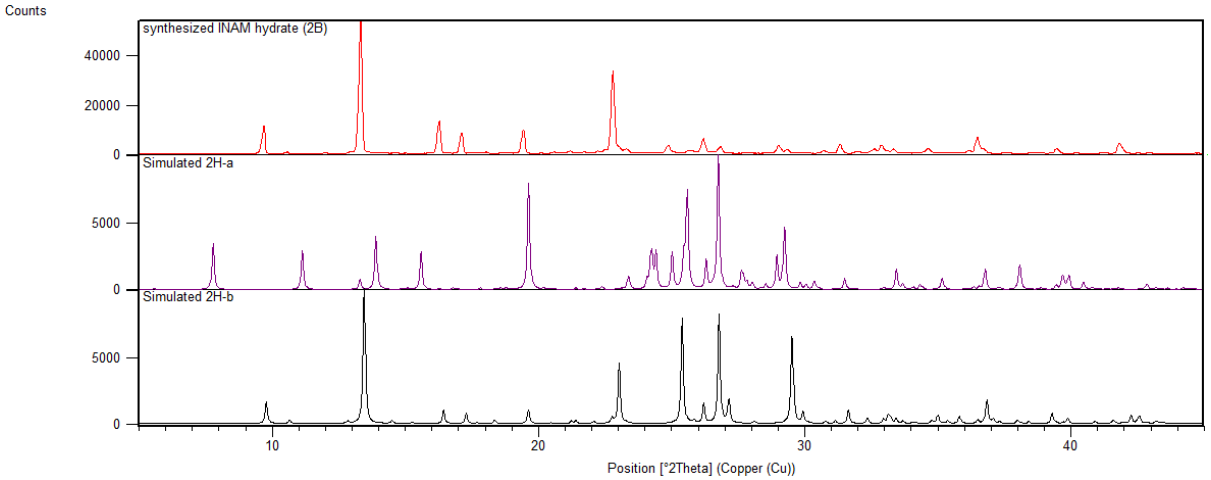

Figure S10. PXRD pattern of synthesised INAM hydrate **2B** (red) compared to simulated powder patterns of known forms.

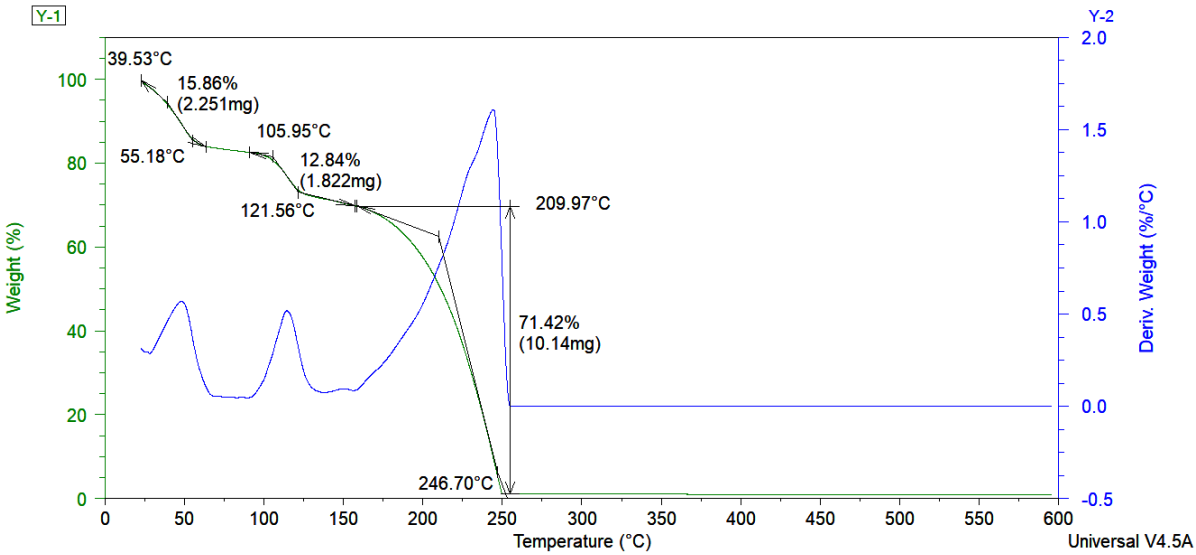

Figure S11. TGA curve of synthesised INAM hydrate (**2B**) with an observed mass loss of 12.84% (calculated mass loss 12.86%). Surface water loss is observed initially.

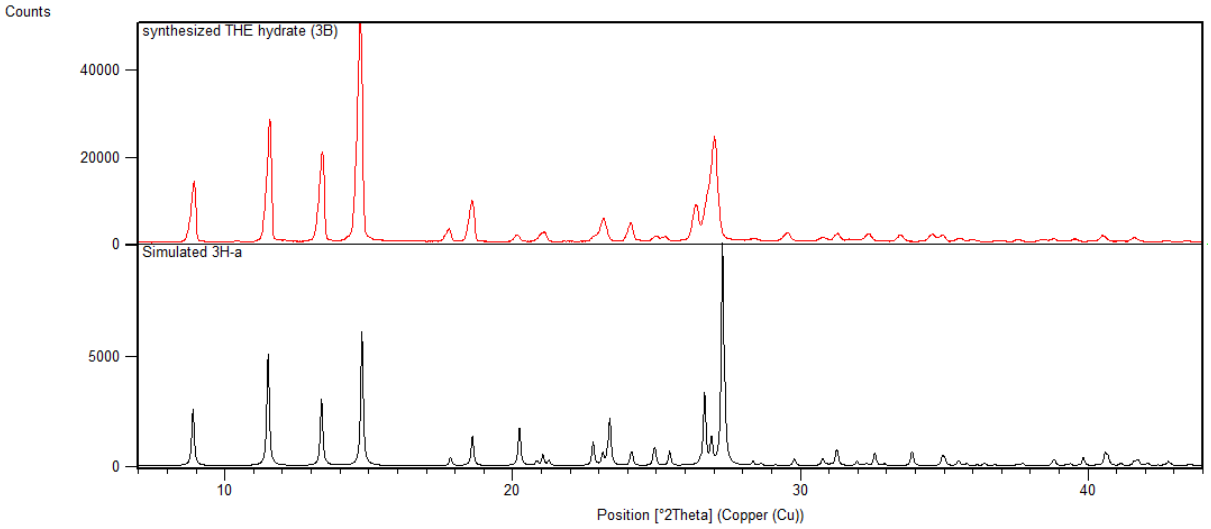

Figure S12. PXRD pattern of synthesised THE hydrate **3B** (red) compared to the simulated powder pattern for **3H-a**.

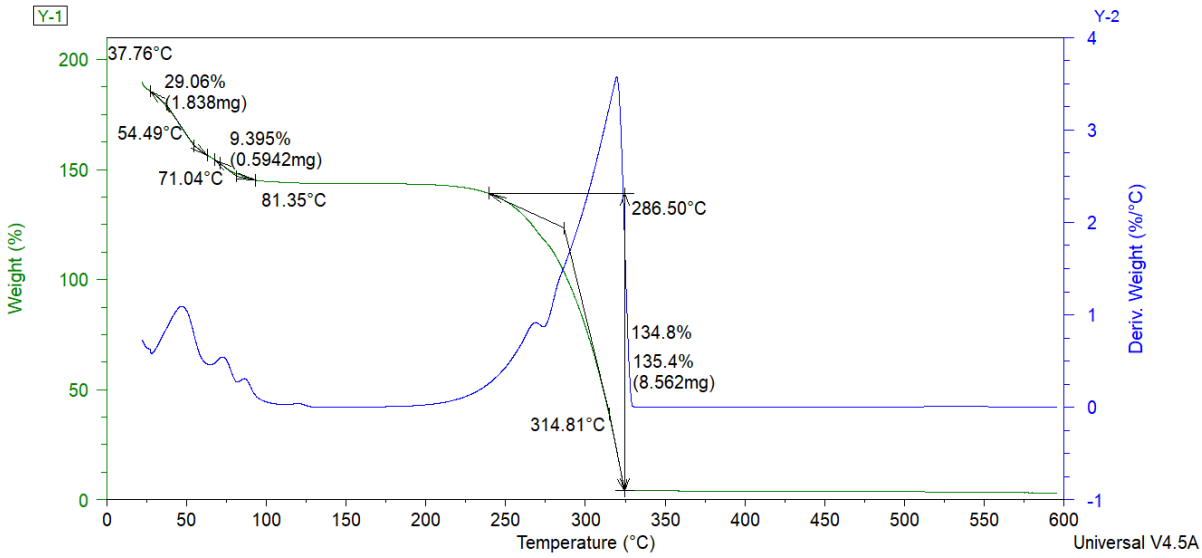

Figure S13. TGA curve of synthesised THE hydrate (**3B**) with a mass loss of 9.40% (calculated mass loss of 9.09% for one water). Surface water loss is observed initially.

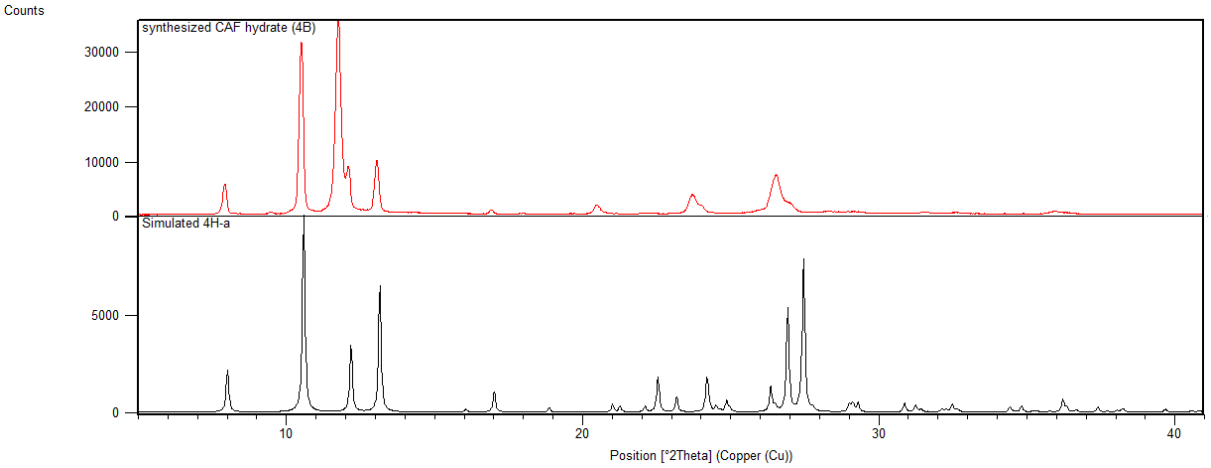

Figure S14. PXRD pattern of synthesised CAF hydrate **4B** (red) compared to simulated powder pattern for **4H-a**.

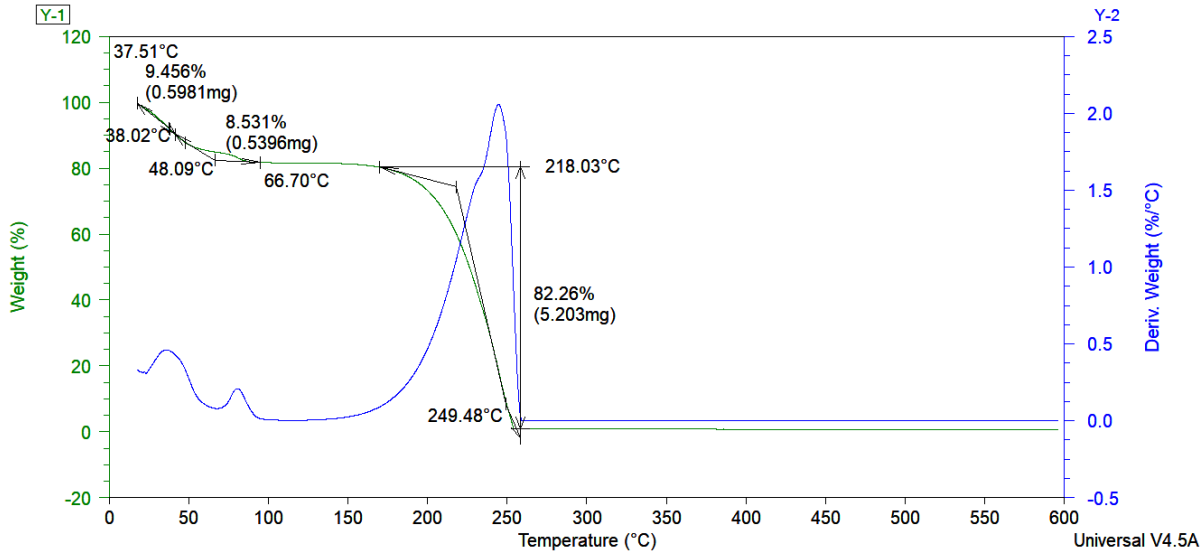

Figure S15. TGA curve of synthesised CAF hydrate (**4B**) with a mass loss of 8.53% water (calculated mass loss of 8.450% for one water). Surface water loss is observed at the start of the heating cycle.

Hydrate stability studies

Stability tests were carried out to assess how fast certain crystal forms lose or accumulate water from the atmosphere. These samples were placed in a 100 ml beaker and exposed to the atmosphere for periods of time. Hydrate stability tests were carried out on hydrate **1**, hydrate **2B**, hydrate **5B**, and anhydrous **5**.

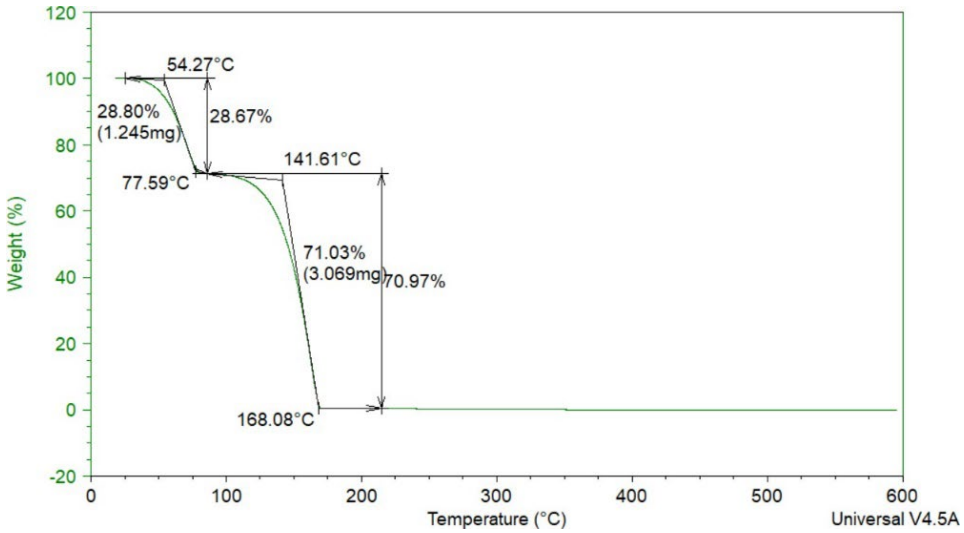

Figure S16. TGA curve of **1** as purchased, with a mass loss of 28.67% (calculated water content 28.58%).

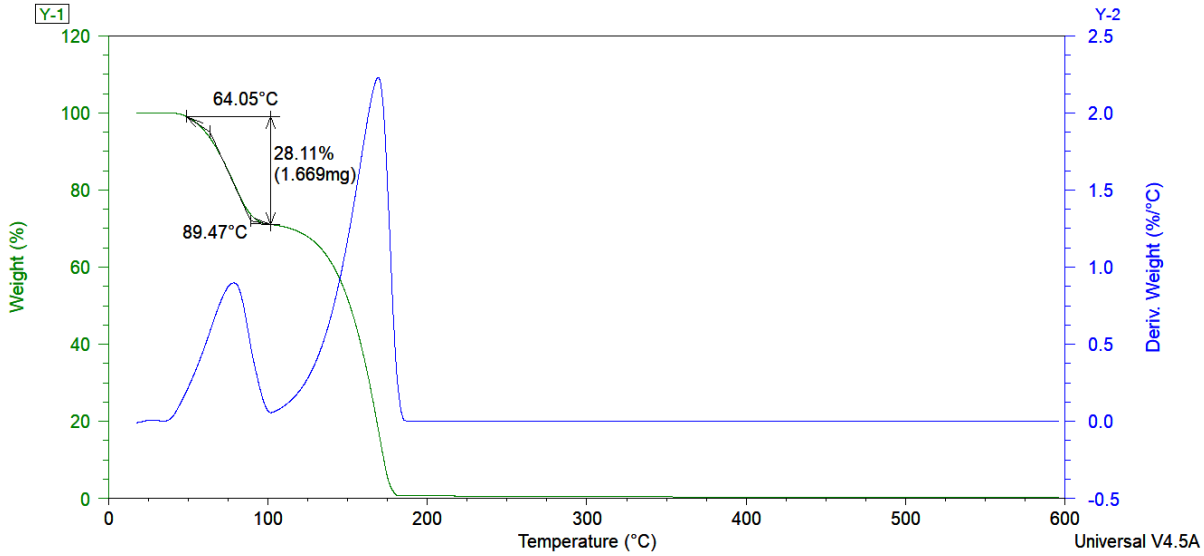

Figure S17. TGA curve of **1** after 1 day exposure to atmosphere, with a mass loss of 28.11%.

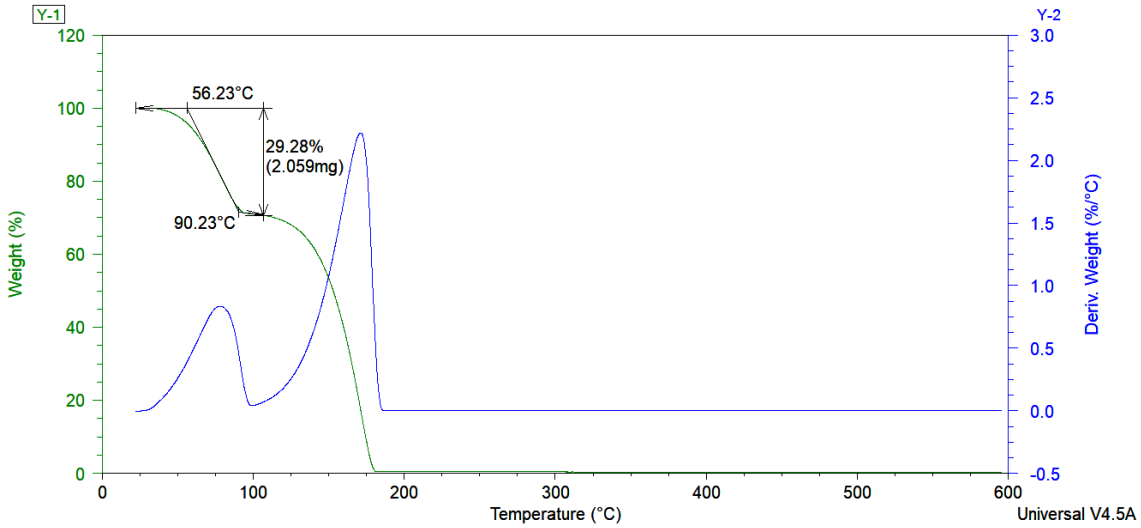

Figure S18. TGA curve of **1** after 9 days of exposure to atmosphere, with a mass loss of 29.28%.

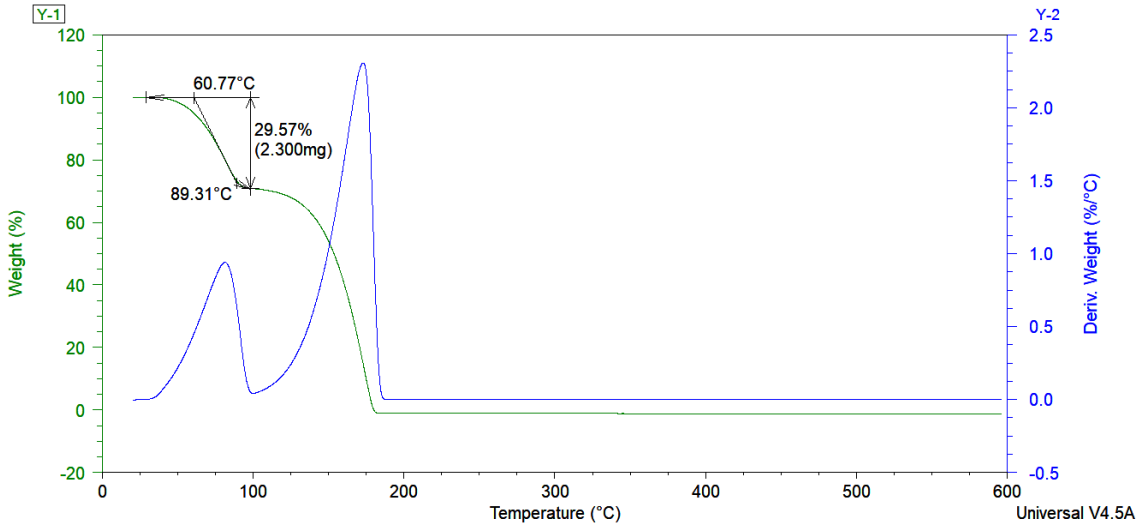

Figure S19. TGA curve of **1** after 14 days of exposure to atmosphere, with a mass loss of 29.57%.

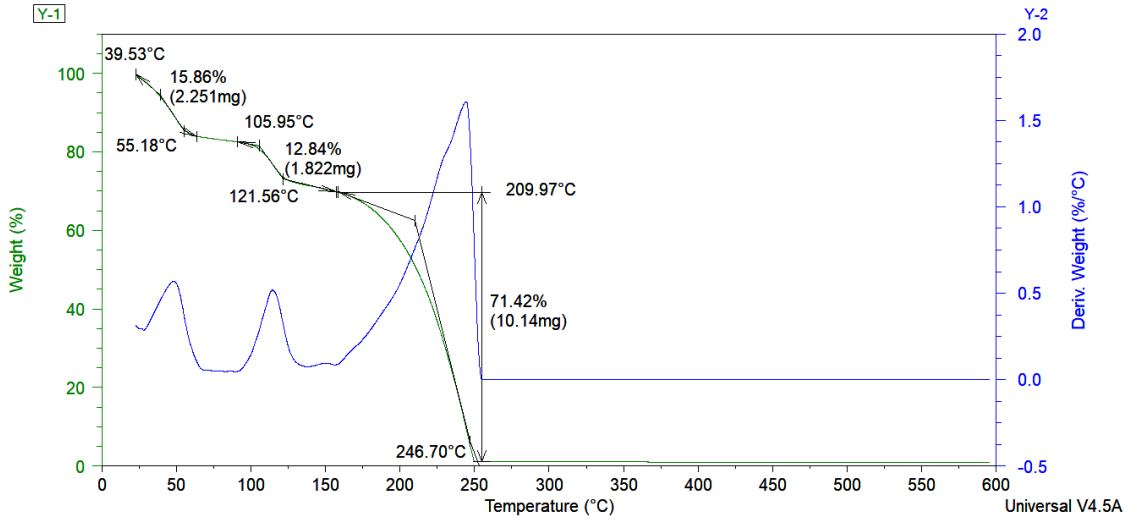

Figure S20. TGA curve of synthesised **2B**, with a mass loss of 12.84% (calculated water content of 12.86%).

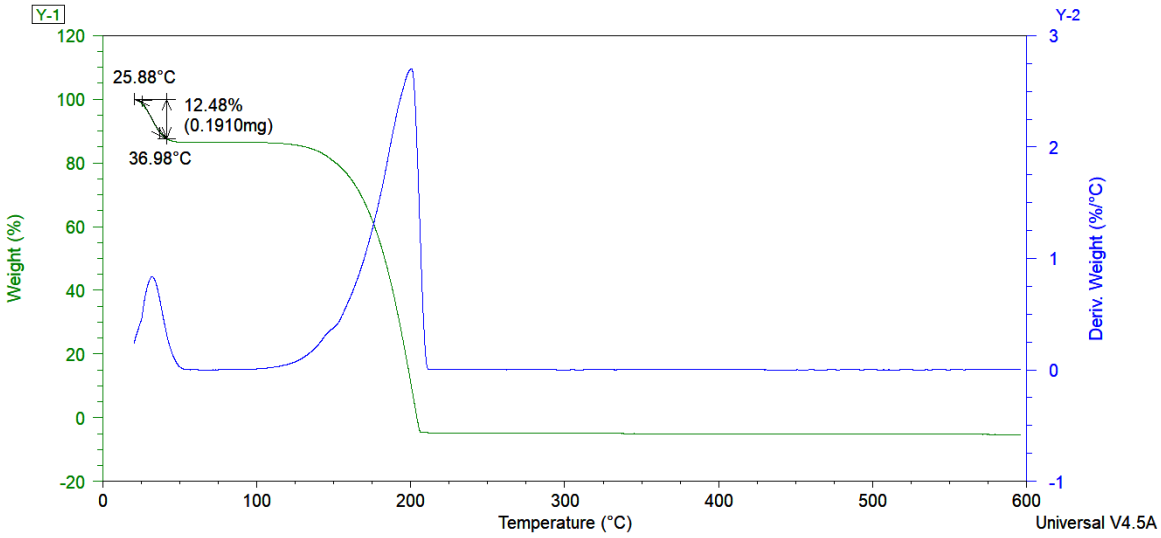

Figure S21. TGA curve of **2B** after 1 day exposure to atmosphere, with a mass loss of 12.48%.

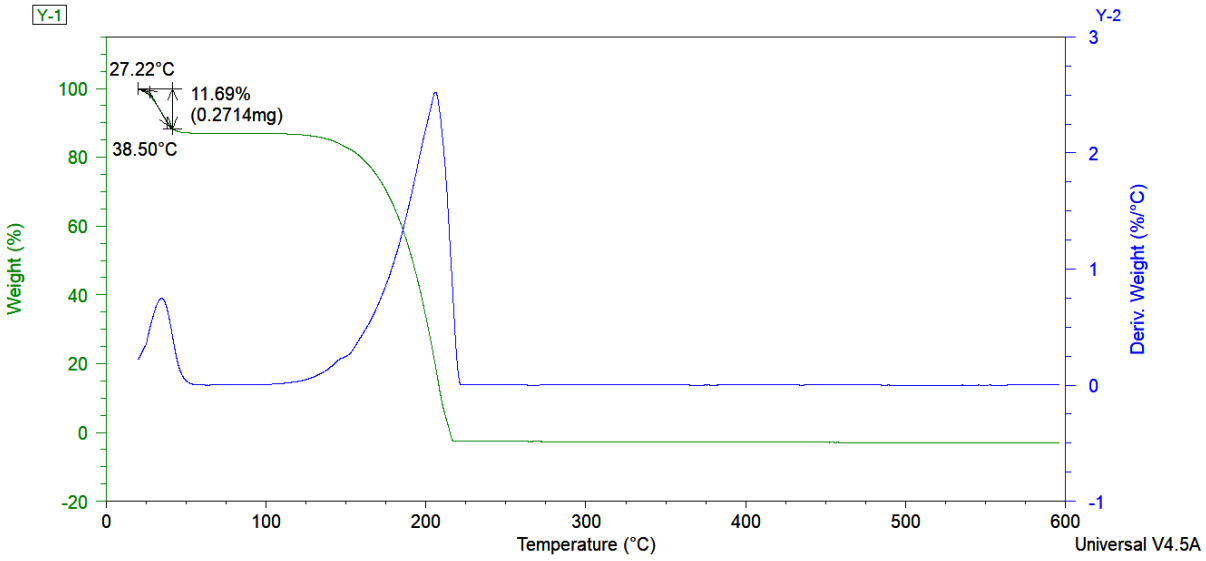

Figure S22. TGA curve of **2B** after 3 days of exposure to atmosphere, with a mass loss of 11.69%.

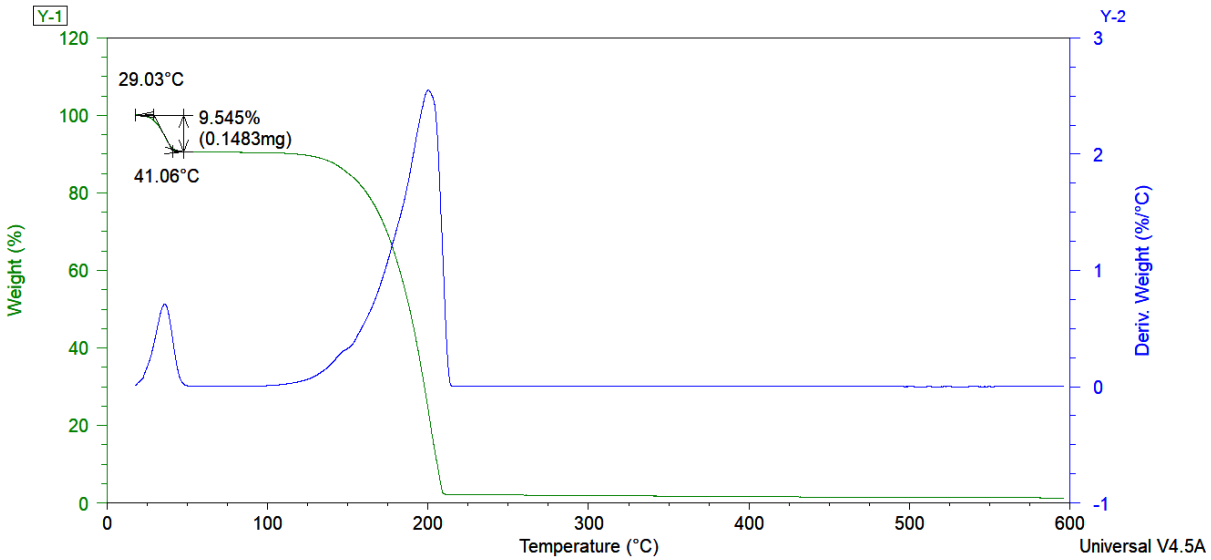

Figure S23. TGA curve of **2B** after 7 days exposure to atmosphere, with a mass loss of 9.545%.

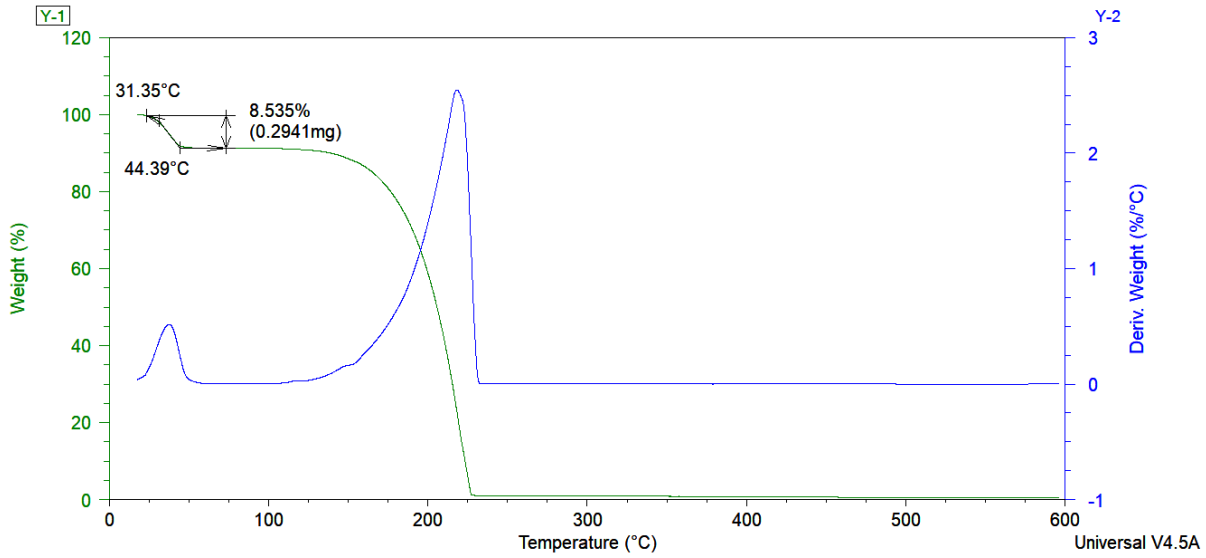

Figure S24. TGA curve of **2B** after 11 days exposure to atmosphere, with a mass loss of 8.535%.

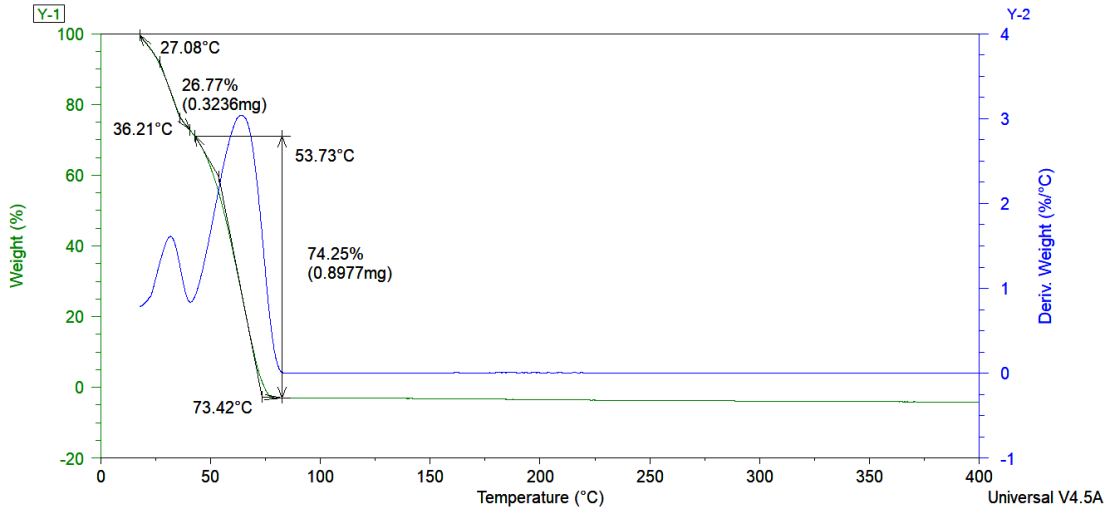

Figure S25. TGA curve of synthesised **5B** with mass loss of 26.77% water (calculated water content of 13.84% for the monohydrate and 49.07% for the hexahydrate).

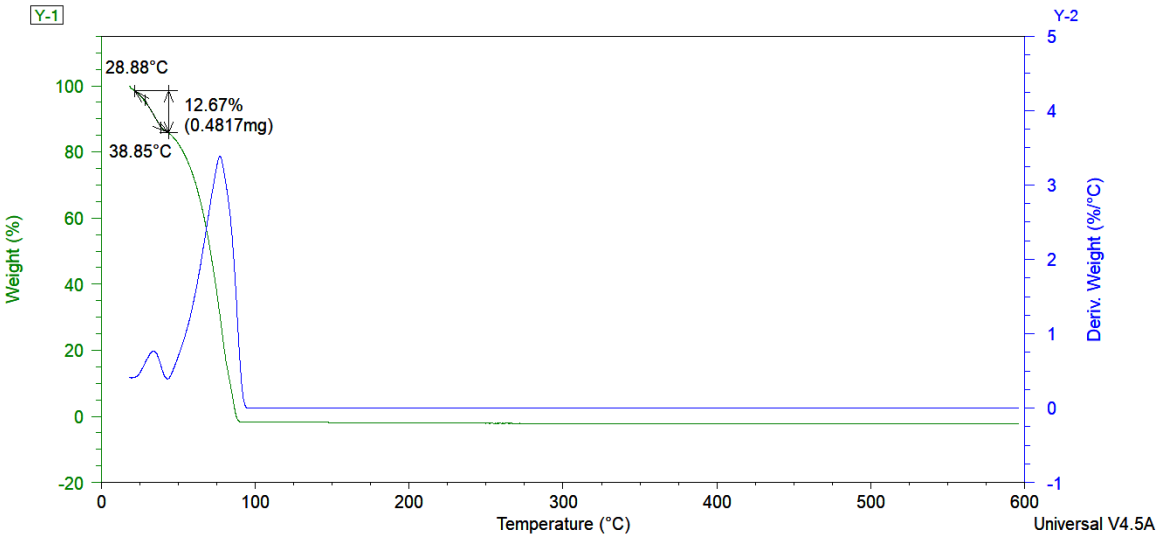

Figure S26. TGA curve of **5B** after 1 day exposure to atmosphere, with mass loss of 12.67%.

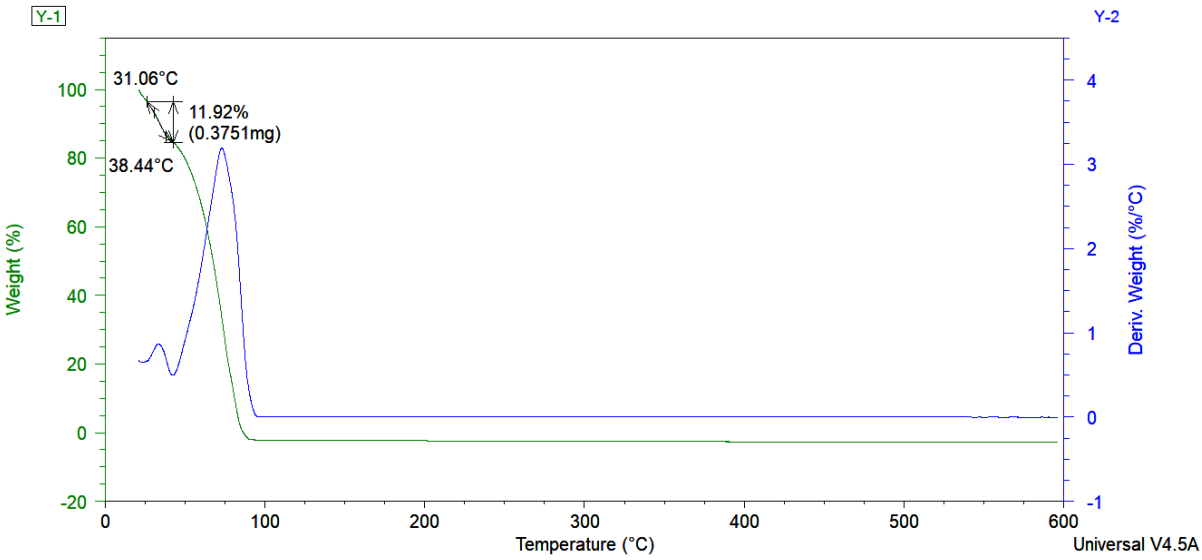

Figure S27. TGA curve of **5B** after 3 days of exposure to atmosphere, with mass loss of 11.92%.

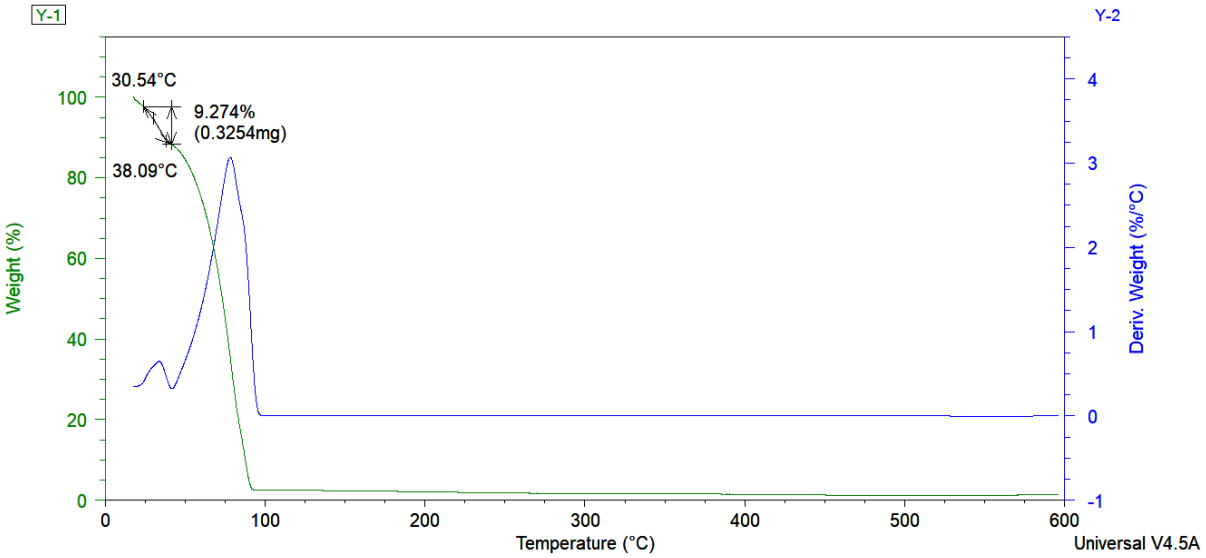

Figure S28. TGA curve of **5B** after 11 days exposure to atmosphere, with a mass loss of 9.274%.

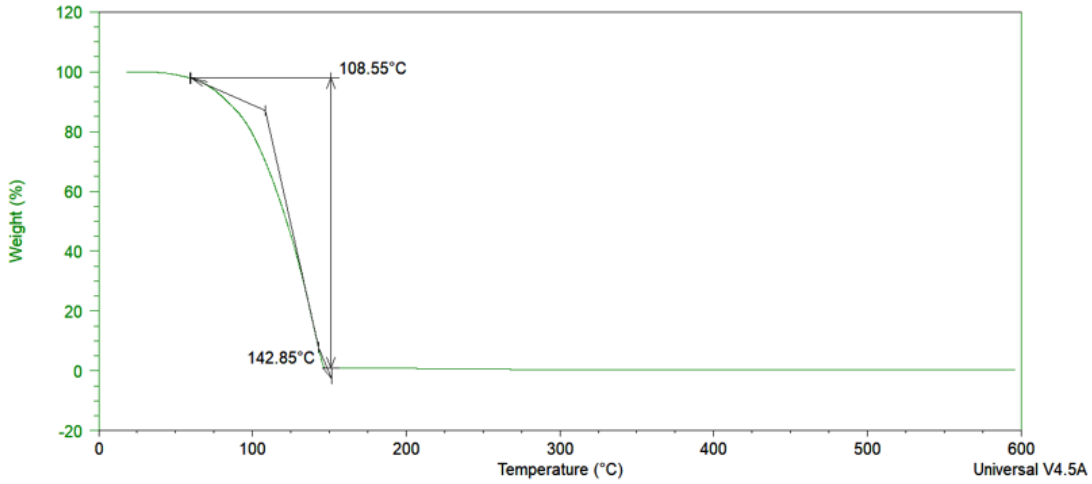

Figure S29. TGA curve of **5** as purchased, with mass loss of 0%.

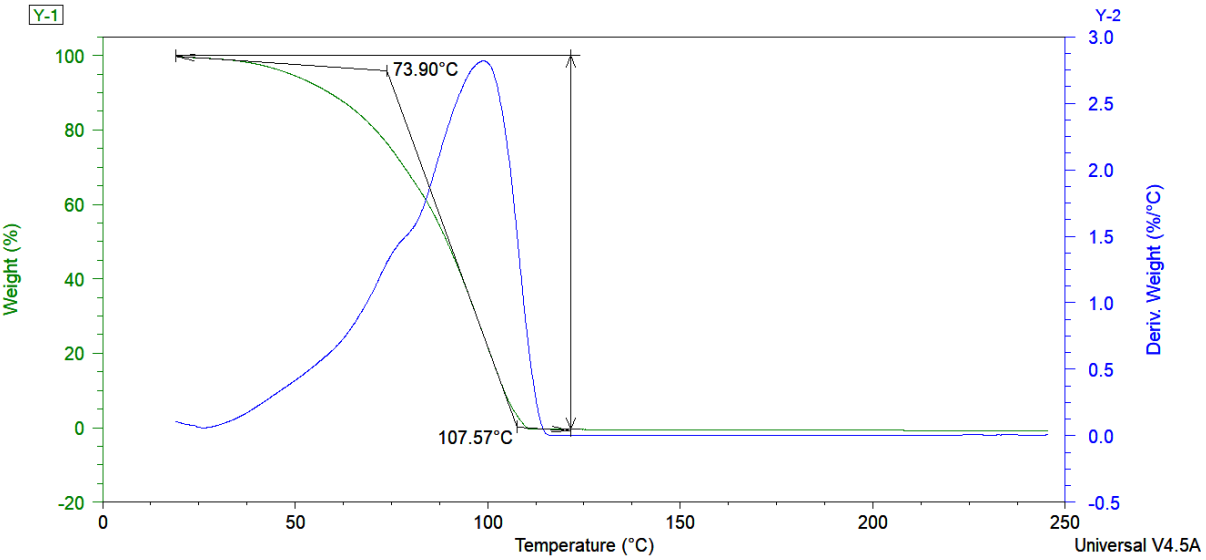

Figure S30. TGA curve of **5** after 3 days exposure to atmosphere, with a mass loss of 0%.

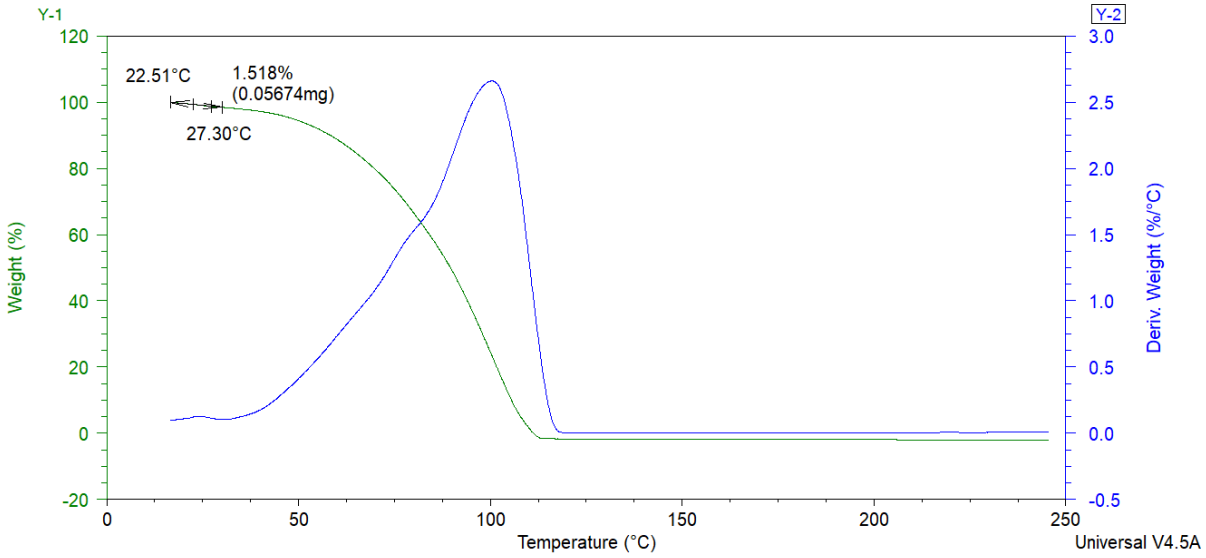

Figure S31. TGA curve of **5** after 11 days exposure to atmosphere, with amass loss of 1.518%.

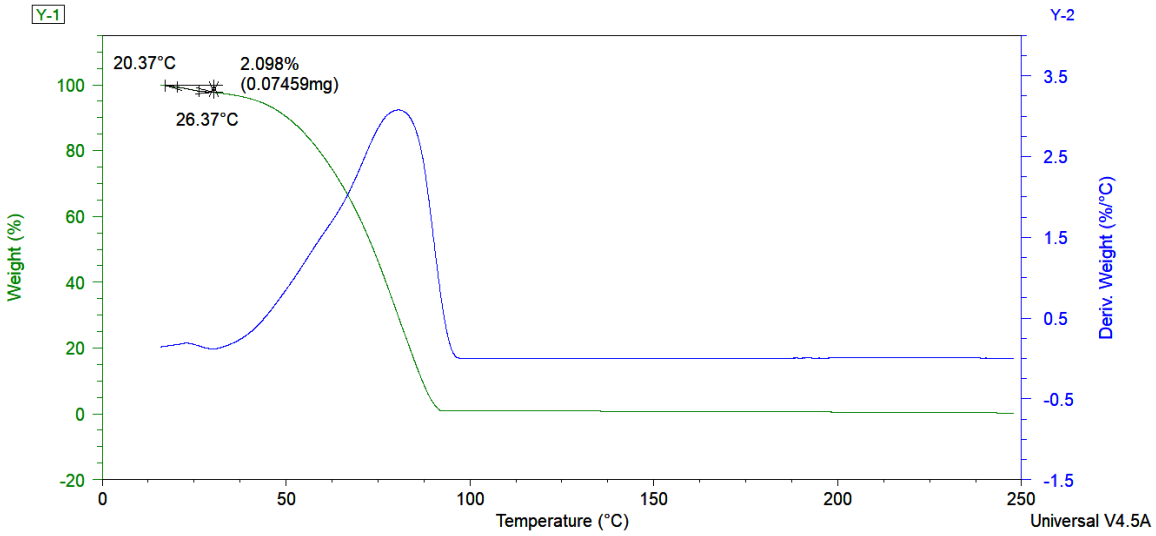

Figure S32. TGA curve of **5** after 18 days exposure to atmosphere, with a mass loss of 2.098%.

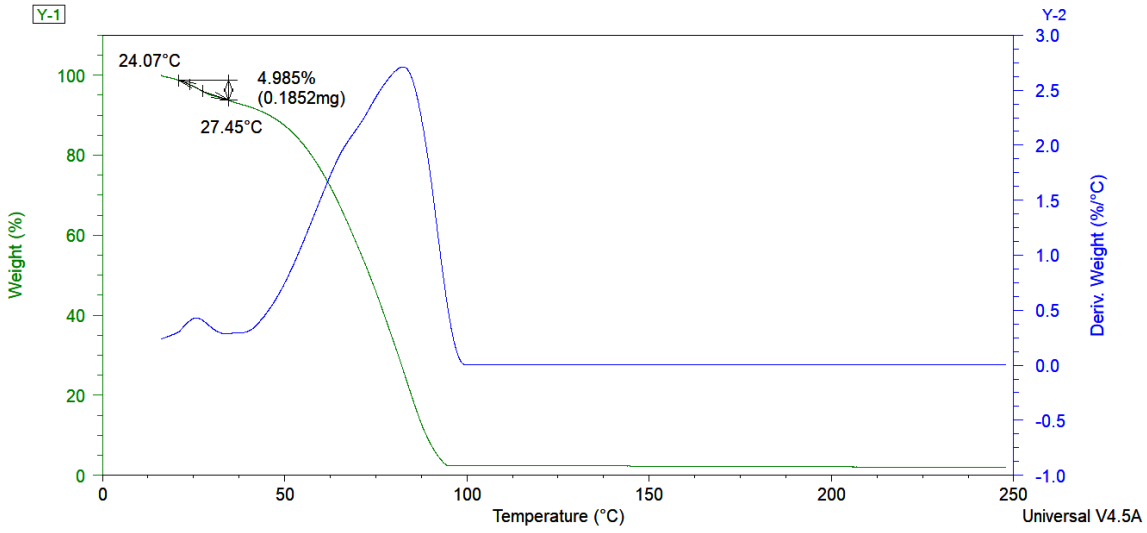

Figure S33. TGA curve of **5** after 28 days exposure to atmosphere, with a mass loss of 4.985%.

Results of sublimation experiments

Table S6 and S7 outline the sublimation conditions and results of the sublimations with anhydrous (S6) and hydrate (S7) forms of compounds **1**-**5** in the presence and absence of water. PXRD and TGA were used as the main analytical techniques, however single-crystal X-ray diffraction (SCXRD) was used in some cases where initial analyses were found inconclusive (Table S9). The sublimation results are followed by the corresponding supporting PXRD and TGA data.

Sublimation experiments highlighted in orange were carried out at least twice, in order to confirm reproducibility of results. During the course of this study, the vacuum pump used initially became unavailable. Having established from other work in our group that vacuum pressure plays a large role in multicomponent crystal growth from the gas phase, the remaining sublimation experiments were not repeated, because it would have been very challenging to obtain the exact vacuum pressure conditions used initially to enable repetition of the experiments under the same conditions for comparative purposes.

Table S6. Results of experiments with **1**-**5** as purchased sublimed in the presence of or excluding water. Note that **1** as purchased is a dihydrate; **2**-**4** are anhydrous forms as purchased.

Material	*Sublimation temperature (°C)*	*Crystal form as purchased*	*Crystal form after sublimed*		*Crystal form after sublimed w/ 30 µL water*		*Crystal form after sublimed w/ 40 µL water*	
			Time(h)		Time(h)		Time(h)	
1 (hydrate) (55 mg)	120	**1H-a**	5.5	**1A-a** **1H-a**	2.5	**1H-a**		
2 (57 mg)	110	**2A-a** **2A-b**	4.5	**2A-a** **2A-b**	8	**2A-a**	55	**2A-a**
3 (58 mg)	150	**3A-a**	20	**3A-a**	15.5	**3A-a** **3H-a**	97	**3A-a**
4 (58 mg)	120	**4A-b**	7	**4A-b**	24	**4A-b**	72	**4A-b**
5 (50 mg)	50	**5A-a**	24	**5A-a**	24	**5A-a** **5B**	24	**5A-a** **5B**

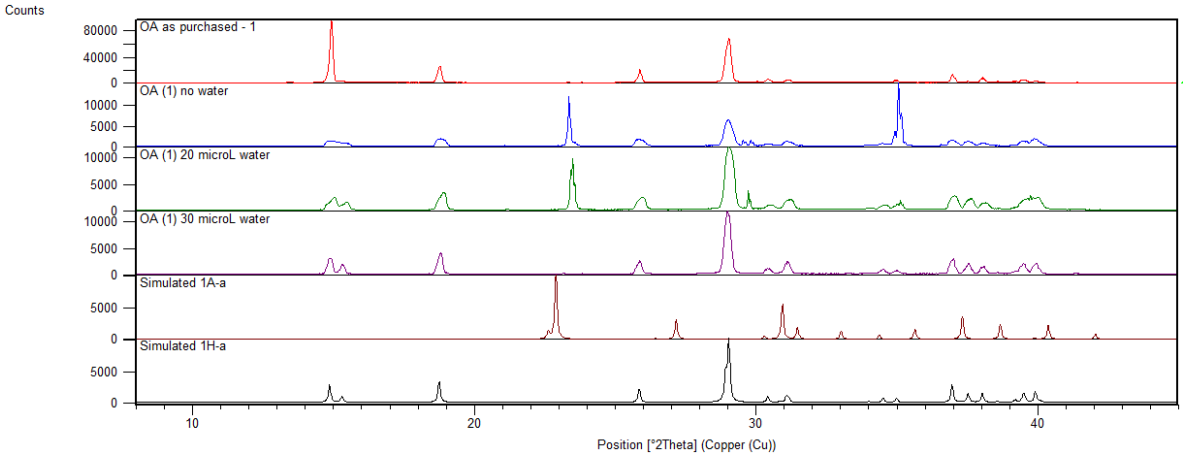

Figure S34. Experimental PXRD pattern of **1** as purchased (red), **1** sublimed without water (blue), **1** sublimed with 20 µL water (green), and **1** sublimed with 30 µL water (purple), compared to simulated patterns.

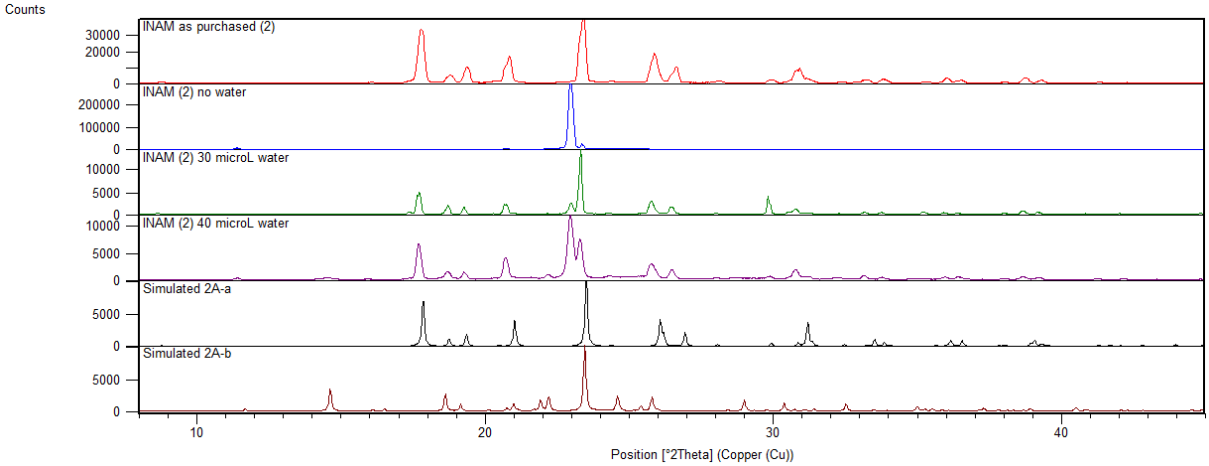

Figure S35. Experimental PXRD pattern of **2** as purchased (red), **2** sublimed without water (blue), **2** sublimed with 30 µL water (green), and **2** sublimed with 40 µL water (purple), compared to simulated patterns.

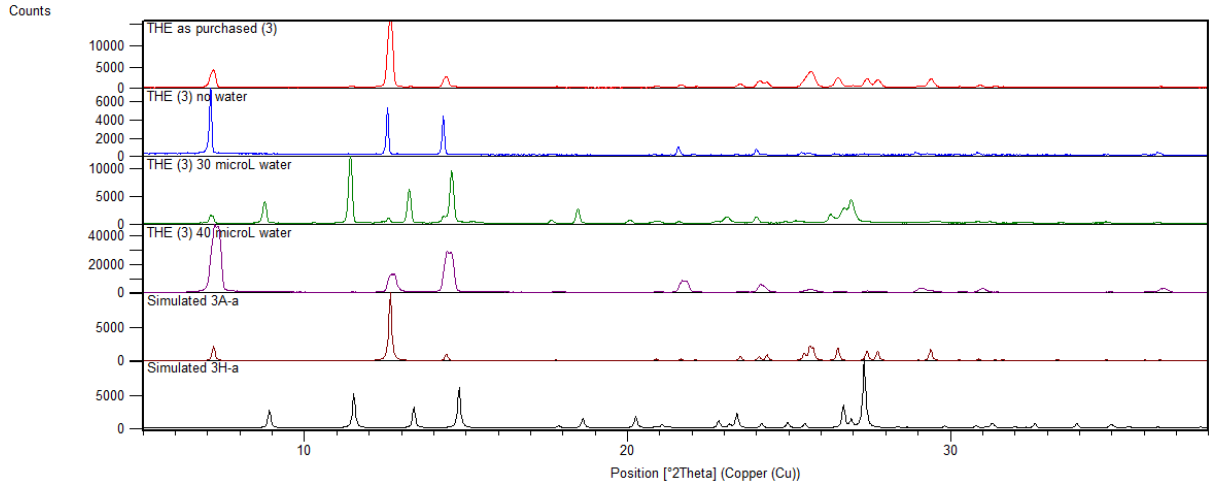

Figure S36. Experimental PXRD pattern of **3** as purchased (red), **3** sublimed without water (blue), **3** sublimed with 30 µL water (green), and **3** (ground) sublimed with 40 µL water (purple), compared to simulated patterns.

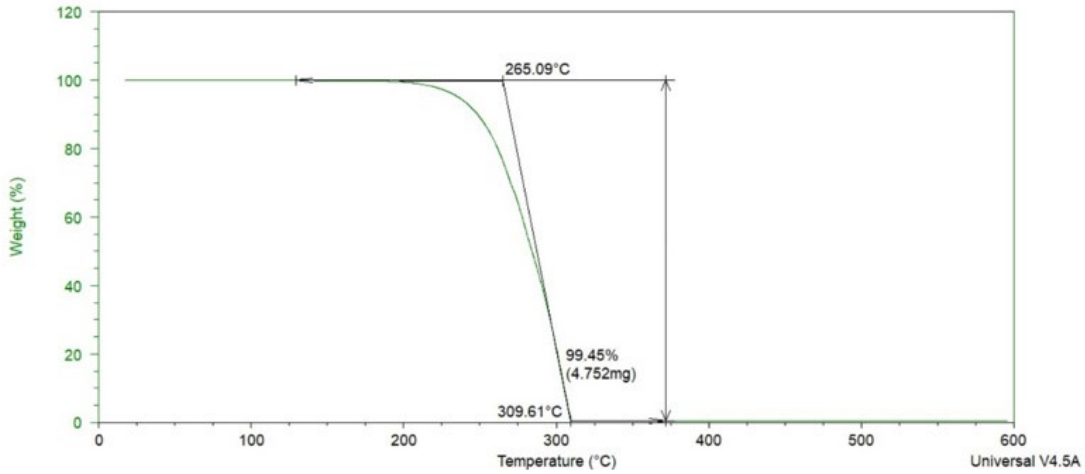

Figure S37.TGA curve of **3** as purchased with an observed mass loss of 0% water.

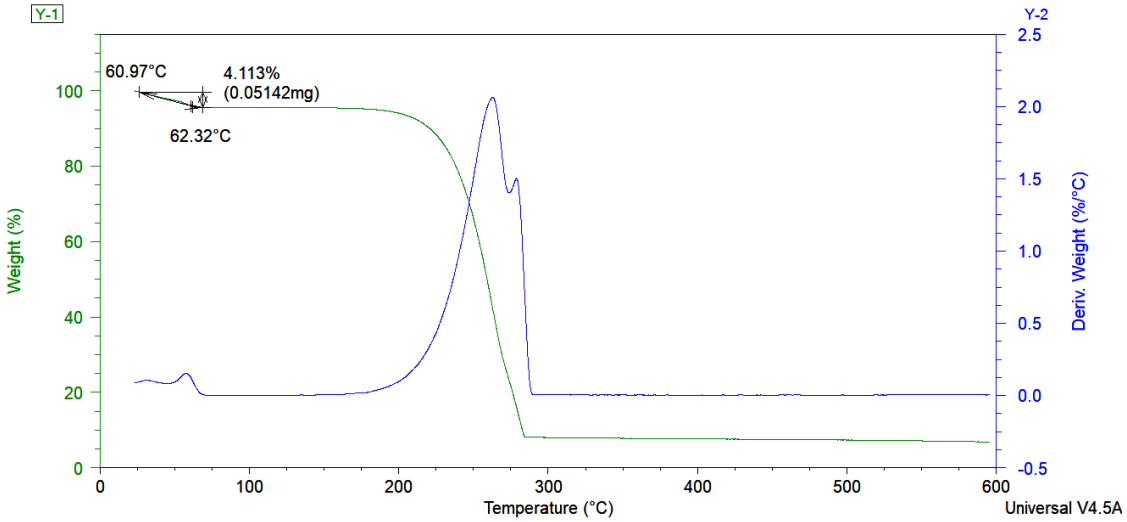

Figure S38. TGA curve of crystals obtained from co-sublimation of **3** with 30 µL water, with an observed mass loss of 4.11%. The sublimation and decomposition of the crystal sample took place concurrently.

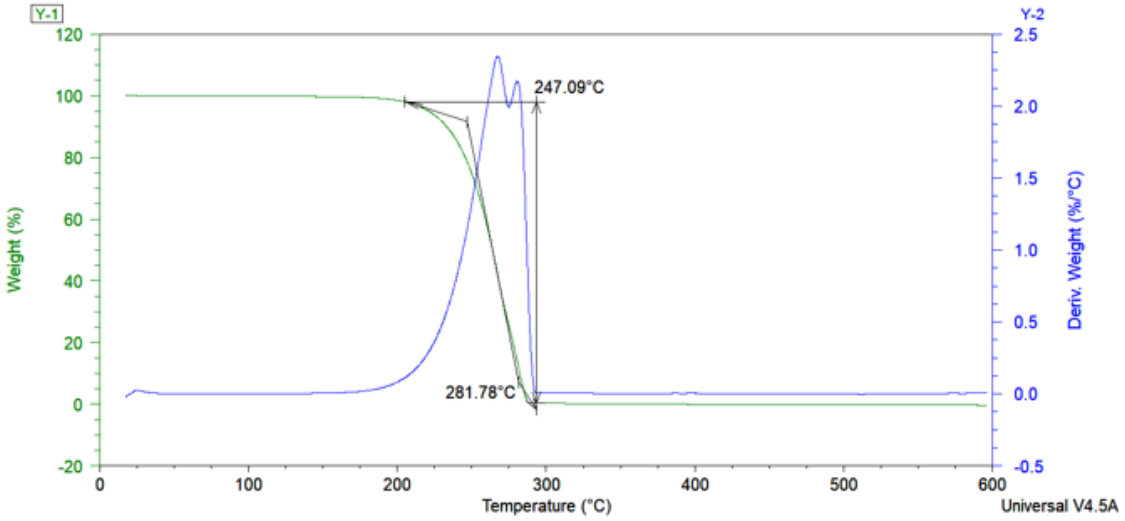

Figure S39. TGA curve of crystals obtained from co-sublimation of **3** with 40 µL water, with an observed mass loss of 0% . The sublimation and decomposition of the crystal sample took place concurrently.

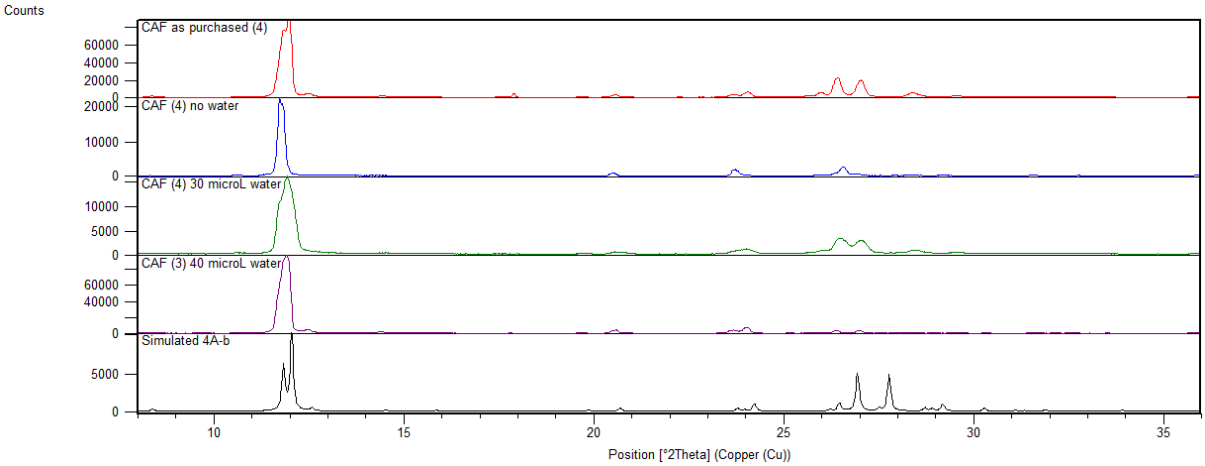

Figure S40. Experimental PXRD pattern of **4** as purchased (red), **4** sublimed without water (blue), **4** sublimed with 30 µL water (green), and **4** sublimed with 40 µL water (purple), compared to simulated patterns.

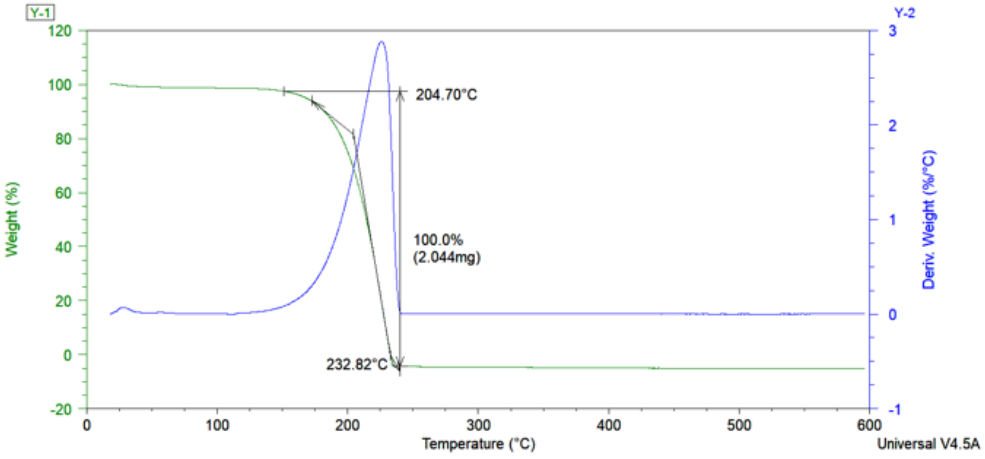

Figure S41. TGA curve of crystals obtained from co-sublimation of **4** with 30 µL water, with an observed mass loss of 0%.

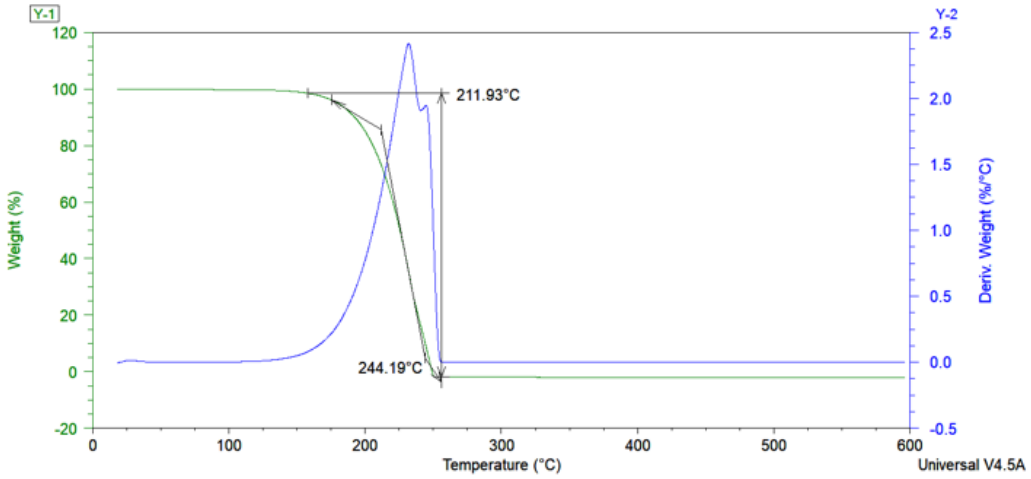

Figure S42. TGA curve of crystals obtained from co-sublimation of **4** with 40 µL water, with an observed mass loss of 0%.

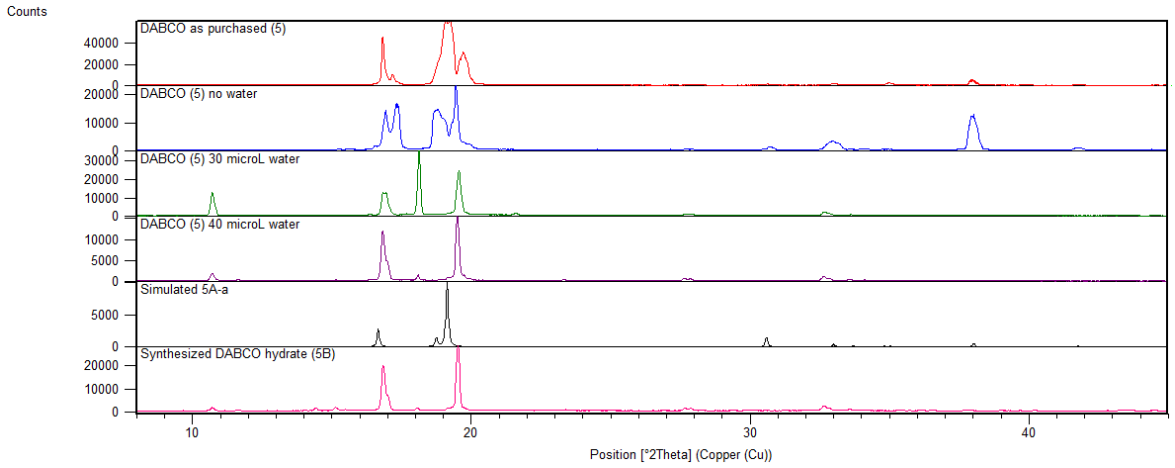

Figure S43. Experimental PXRD pattern of **5** as purchased (red), **5** sublimed without water (blue), **5** sublimed with 30 µL water (green), and **5** sublimed with 40 µL water (purple), compared to simulated patterns.

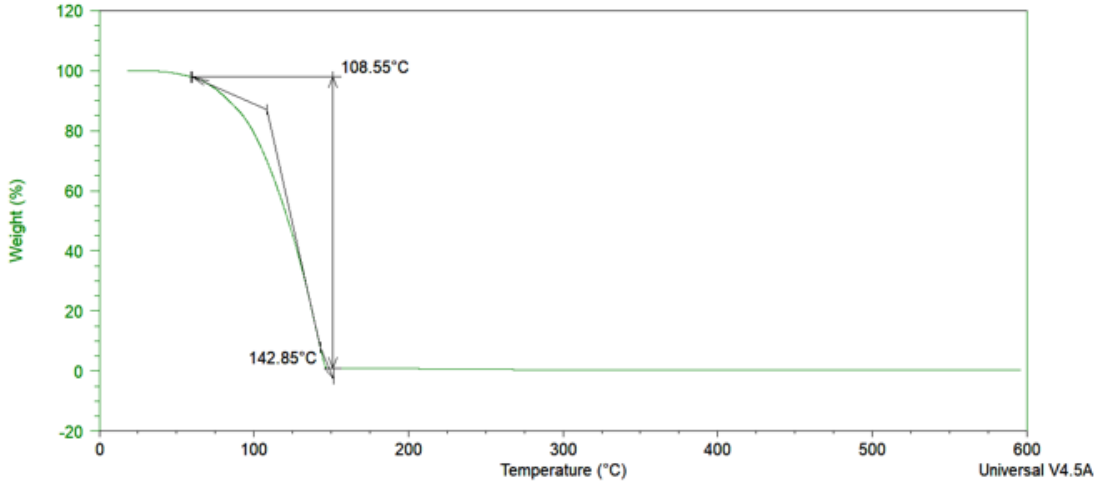

Figure S44. TGA curve of **5** as purchased, with a 0% mass loss.

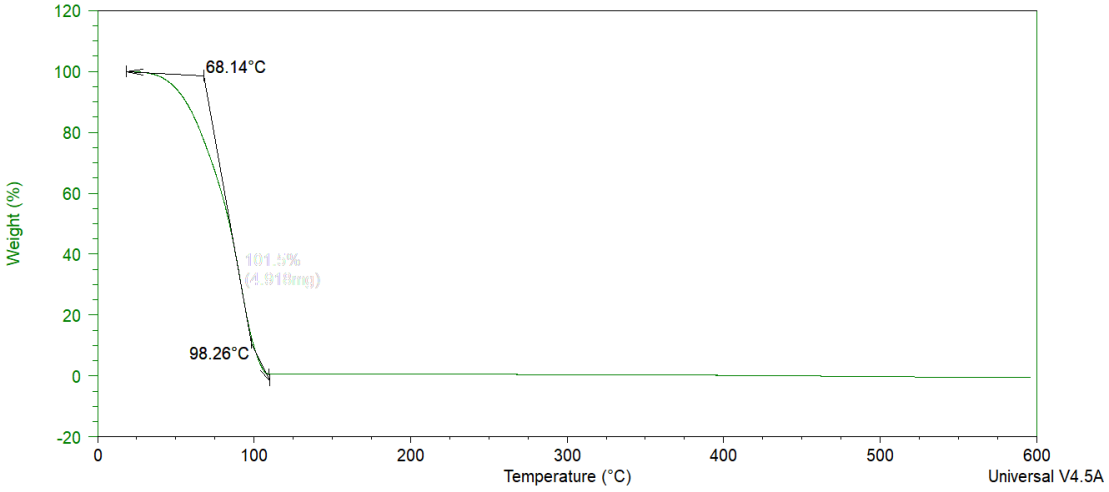

Figure S45. TGA curve of crystals obtained from sublimation of **5** without water, with a 0% mass loss.

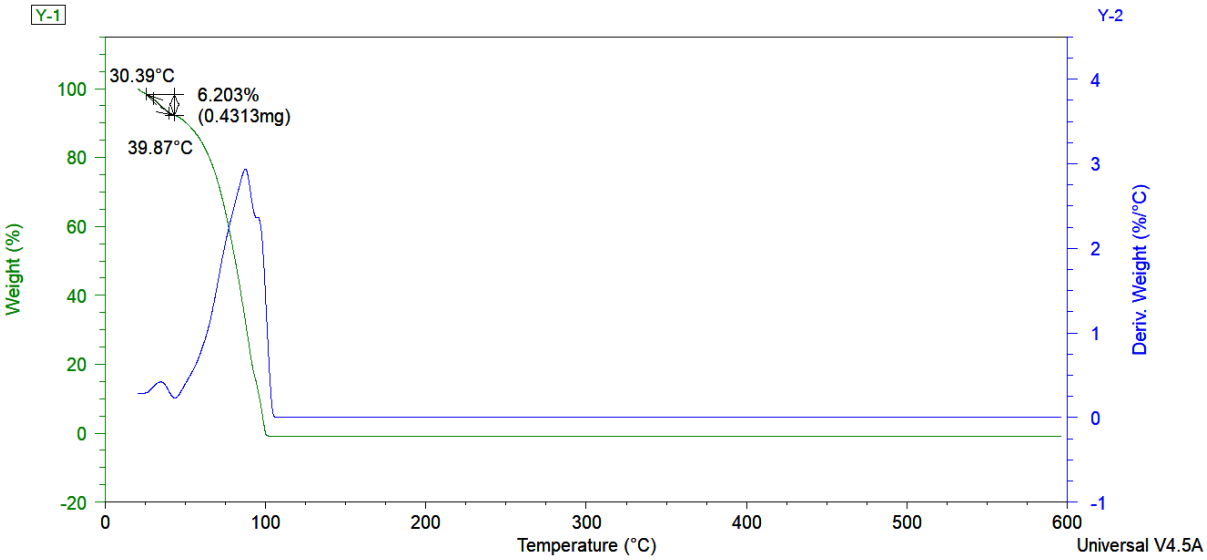

Figure S46. TGA curve of crystals obtained from co-sublimation of **5** with 30 µL water, with an observed mass loss of 6.20%. The sublimation and decomposition of the crystal sample took place concurrently.

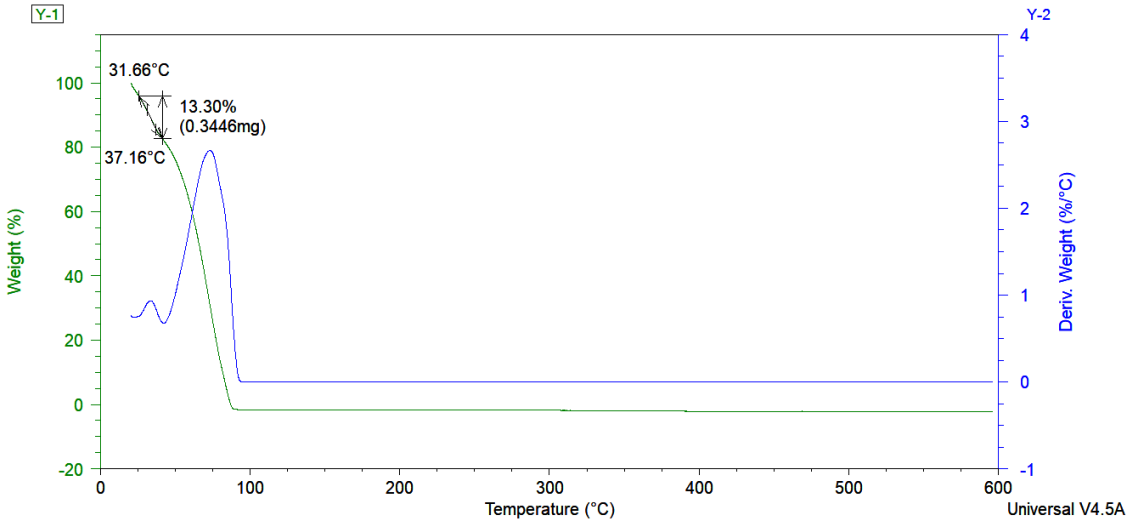

Figure S47. TGA curve of crystals obtained from co-sublimation of **5** with 40 µL water, with an observed mass loss of 13.30%.

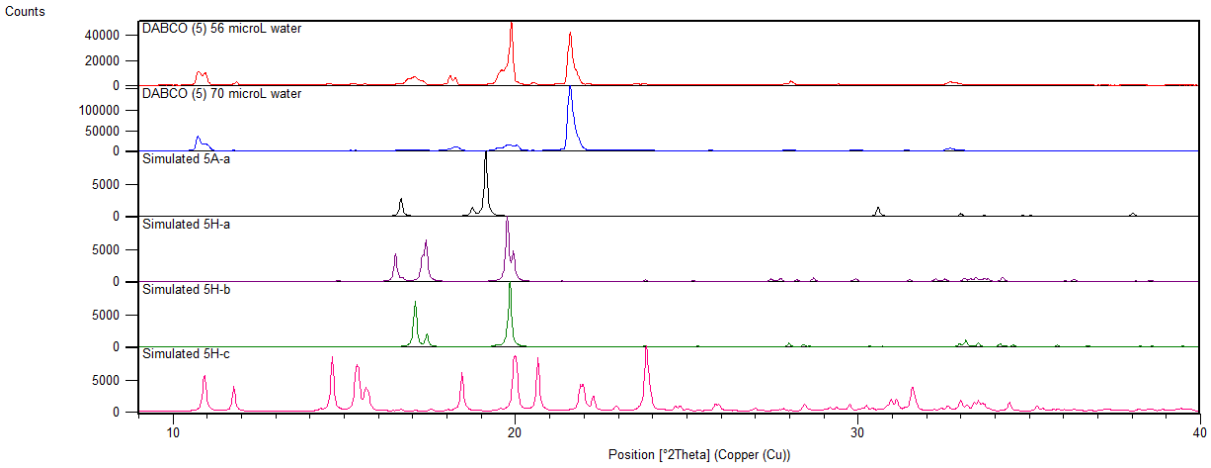

Figure S48. Experimental PXRD pattern of **5** sublimed with 56 µL water (red), **5** sublimed with 70 µL water (blue), compared to simulated patterns.

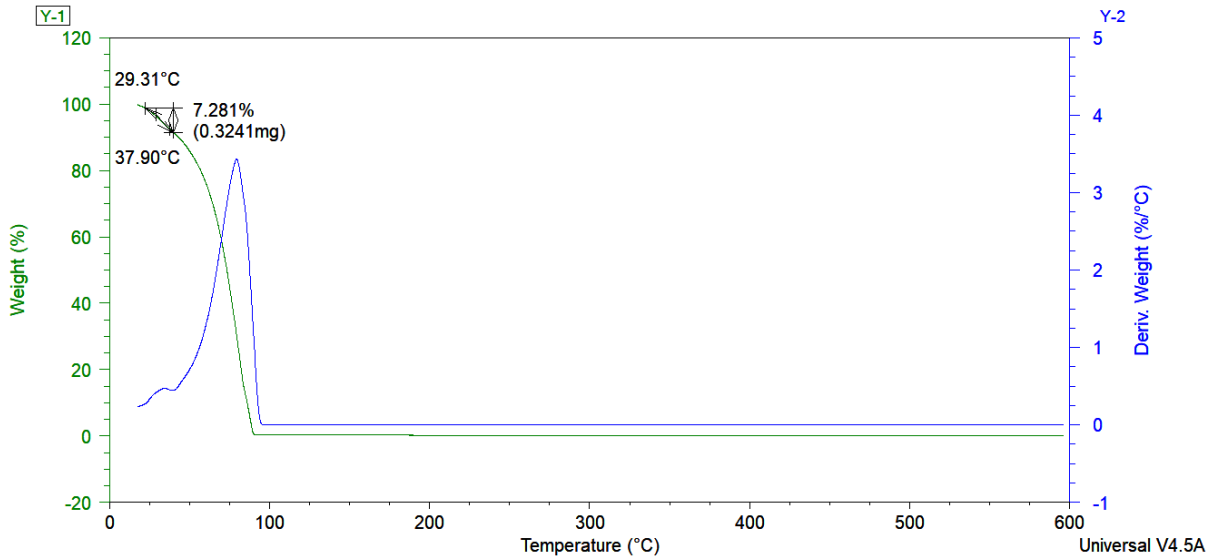

Figure S49. TGA curve of crystals obtained from co-sublimation of **5** with 56 µL water, with an observed mass loss of 7.28%.

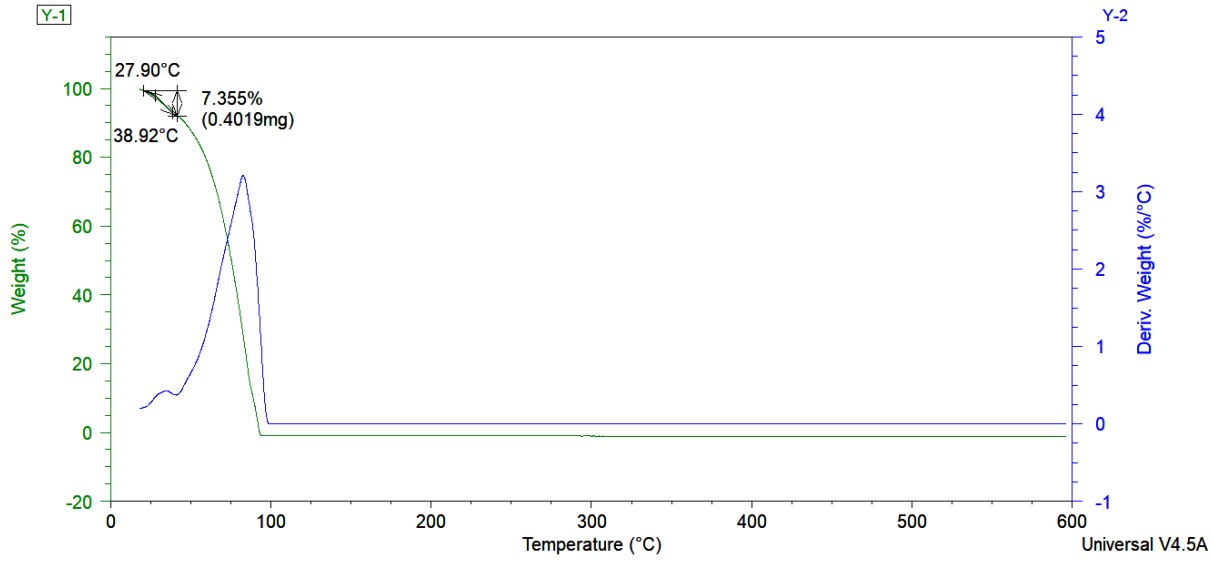

Figure S50. TGA curve of crystals obtained from co-sublimation of **5** with 70 µL water, with an observed mass loss of 7.36%.

Table S7. Results of experiments with synthesised hydrates **2B**, **3B**, **4B**, **5B,** and synthesised anhydrous OA, sublimed in the presence or absence of water.

Material	*Sublimation temperature (°C)*	*Crystal form as synthesised*	*Crystal form after sublimed*		*Crystal form after sublimed w/ 30 µL water*		*Crystal form after sublimed w/ 40 µL water*	
			Time (h)		Time (h)		Time (h)	
1A (used 57 mg **1**)	80	**1A-a** **1A-b**	22	**1A-a** **1A-b** **1H-a**	48.5	**1H-a**	46	**1H-a**
2B (used 58 mg **2**)	110	**2H-b**	68	**2H-a** **2H-b**	33	**2A-a** **2A-b**	89	**2A-a** **2A-b** **2A-c**
3B (used 58 mg **3**)	165	**3H-a**	46	**3A-a**	39	**3A-a**	30	**3A-a**
4B (used 58 mg **4**)	120	**4H-a**	45	**4A-b**	28	**4A-b**	30	**4A-b**
5B (synthesised using adapted literature method[14])	50	**5A-a** **5H-b** **5H-c**	24	**5H-b** **5H-c**	24	**5H-b** **5H-c**	24	**5H-b** **5H-c**

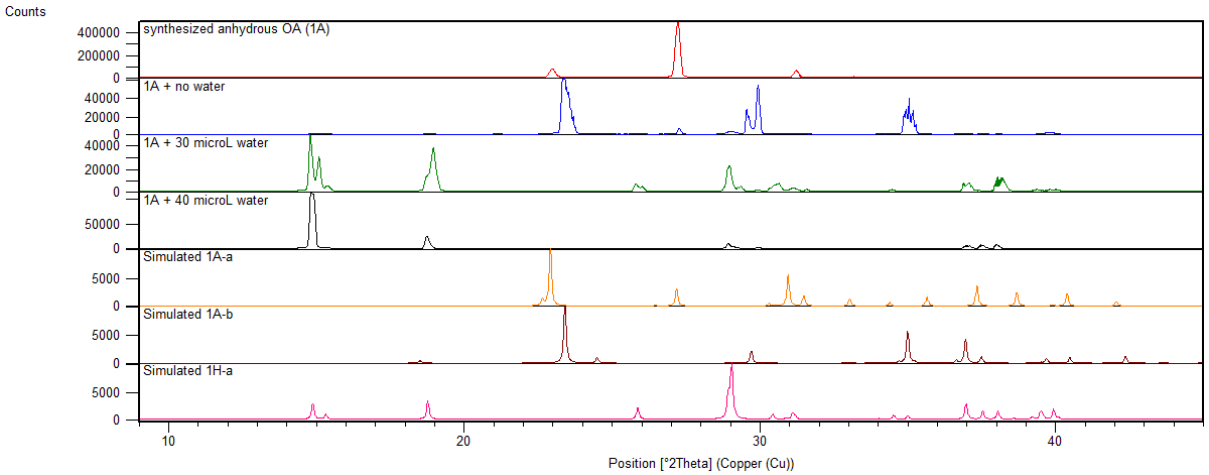

Figure S51. Experimental PXRD pattern of compound **1A** as synthesised (red), **1A** sublimed without water (blue), **1A** sublimed with 30 µL water (green), and **1A** sublimed with 40 µL water (black), compared to simulated patterns.

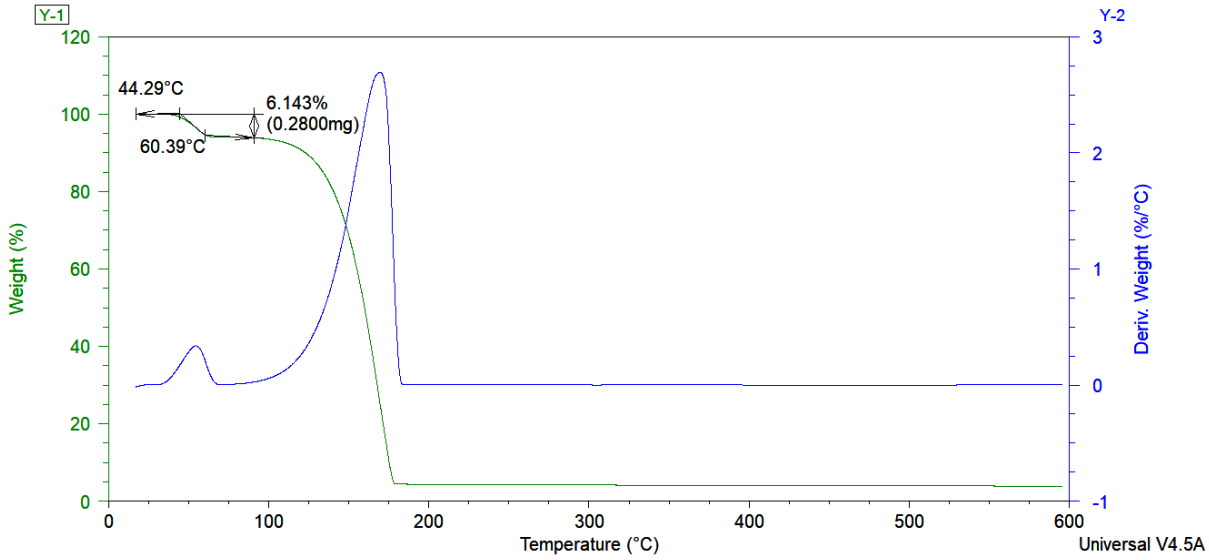

Figure S52. TGA curve of crystals obtained from sublimation of **1A** without water, with an observed mass loss of 6.14%.

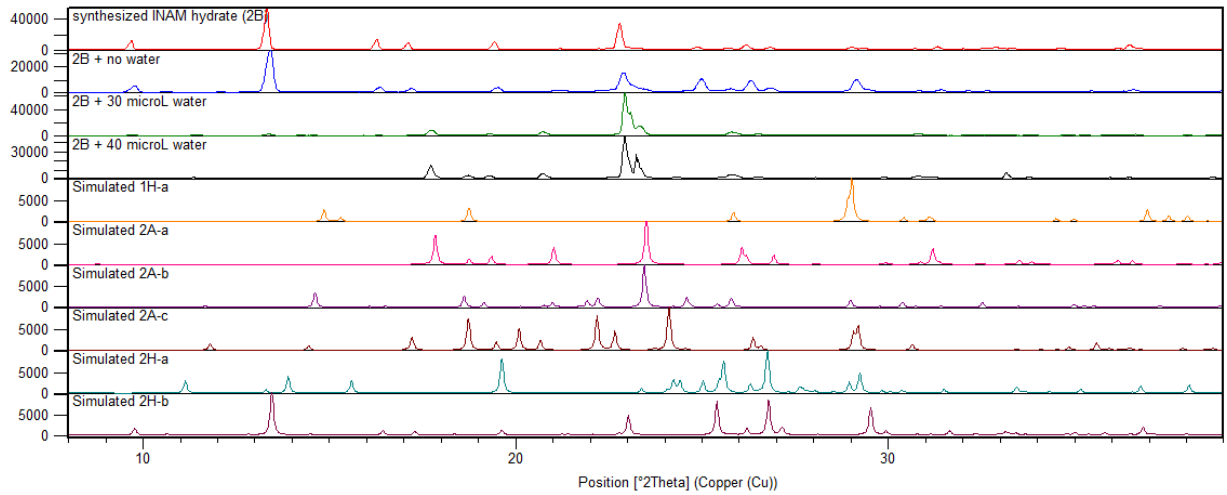

Figure S53. Experimental PXRD pattern of synthesised **2B** (red), **2B** sublimed without water (blue), **2B** sublimed with 30 µL water (green), and **2B** sublimed with 40 µL water (black), compared to simulated patterns.

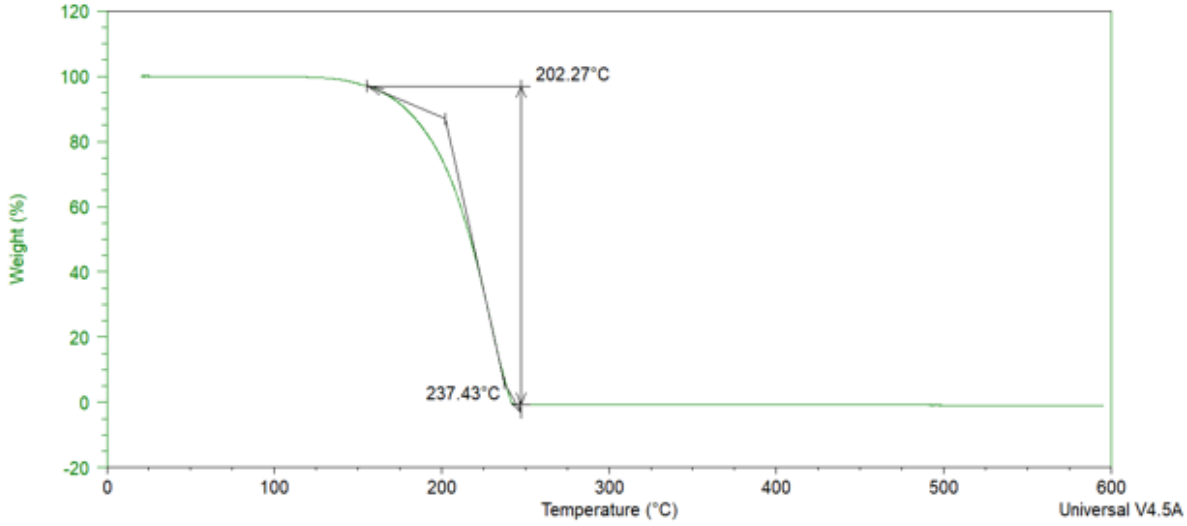

Figure S54. TGA curve of crystals obtained from co-sublimation of **2B** with 30 µL water, with an observed mass loss of 0%.

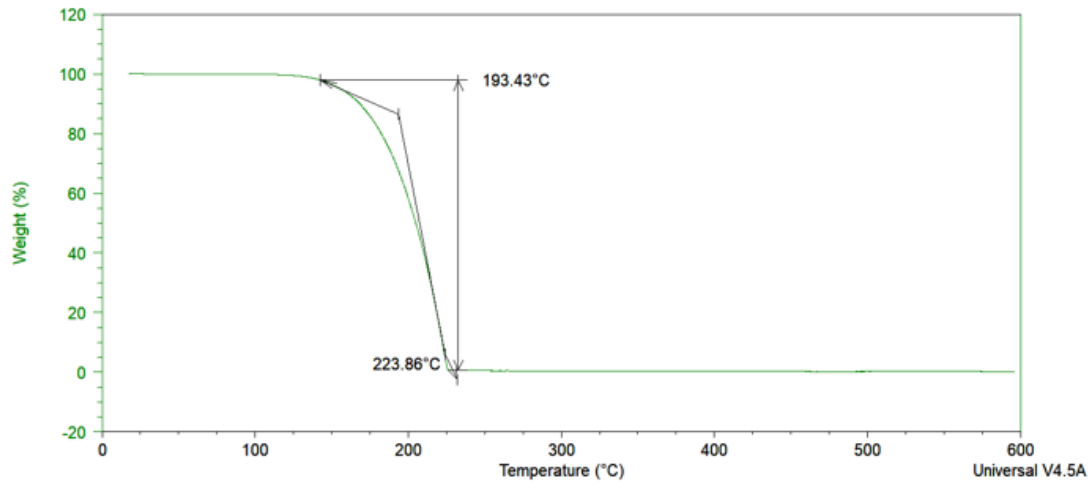

Figure S55. TGA curve of crystals obtained from co-sublimation of **2B** with 40 µL water, with an observed mass loss of 0%.

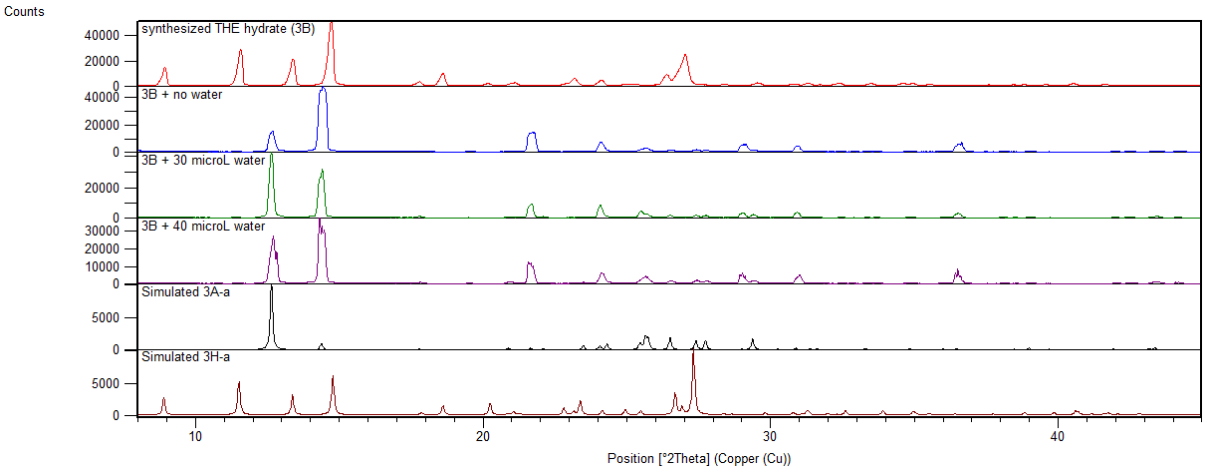

Figure S56. Experimental PXRD pattern of synthesised **3B** (red), **3B** sublimed without water (blue), **3B** sublimed with 30 µL water (green), and **3B** sublimed with 40 µL water (purple), compared to simulated patterns.

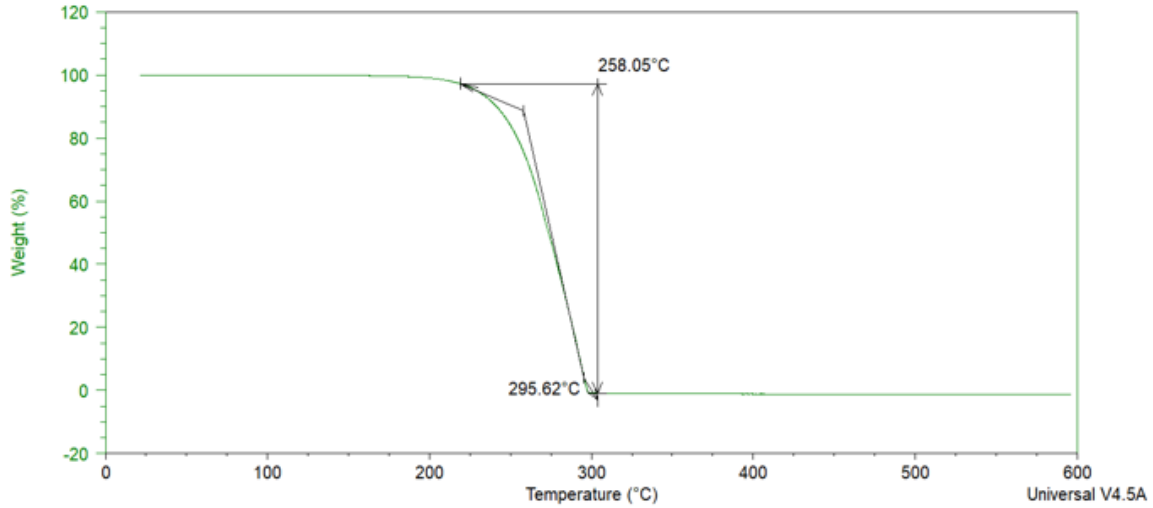

Figure S57. TGA curve of crystals obtained from co-sublimation of **3B** with 30 µL water, with an observed mass loss of 0%.

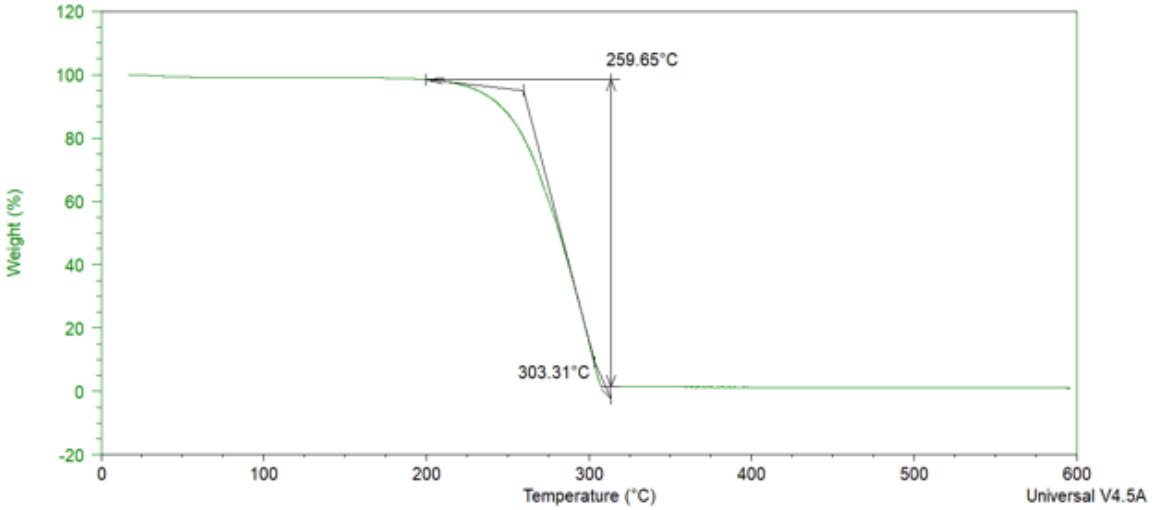

Figure S58. TGA curve of crystals obtained from co-sublimation of **3B** with 40 µL water, with an observed mass loss of 0%.

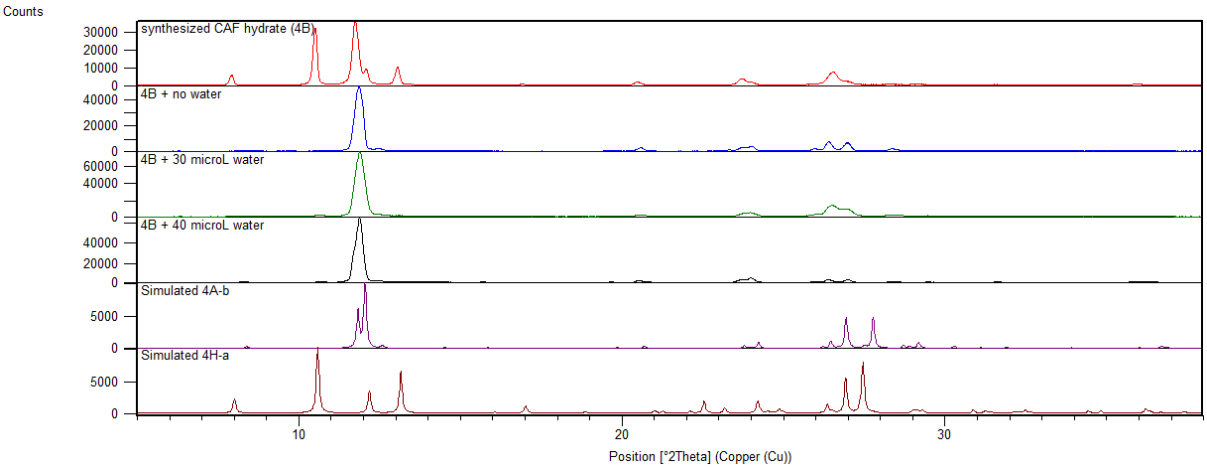

Figure S59. Experimental PXRD pattern of synthesised **4B** (red), **4B** sublimed without water (blue), **4B** sublimed with 30 µL water (green), and **4B** sublimed with 40 µL water (black), compared to simulated patterns.

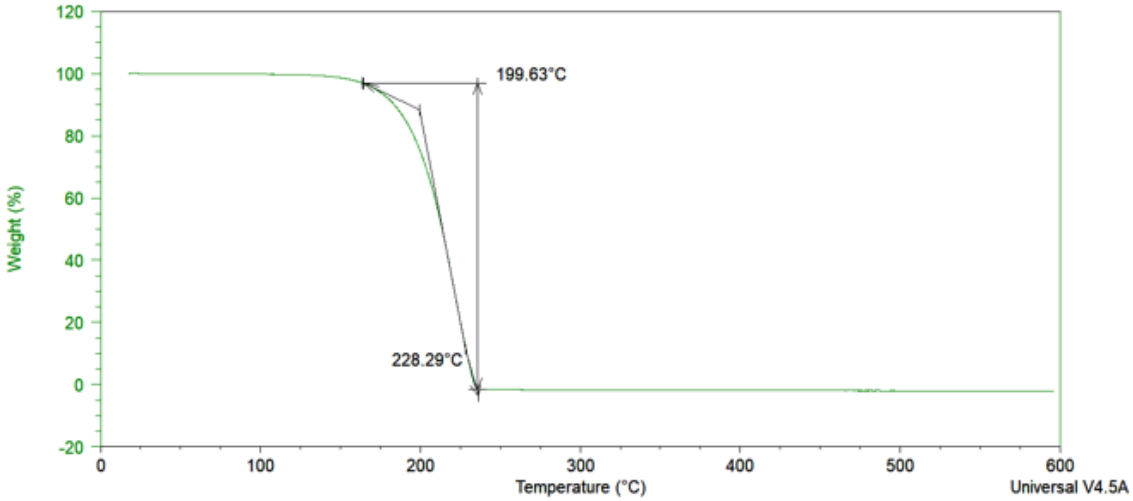

Figure S60. TGA curve of crystals obtained from co-sublimation of **4B** with 30 µL water, with an observed mass loss of 0%.

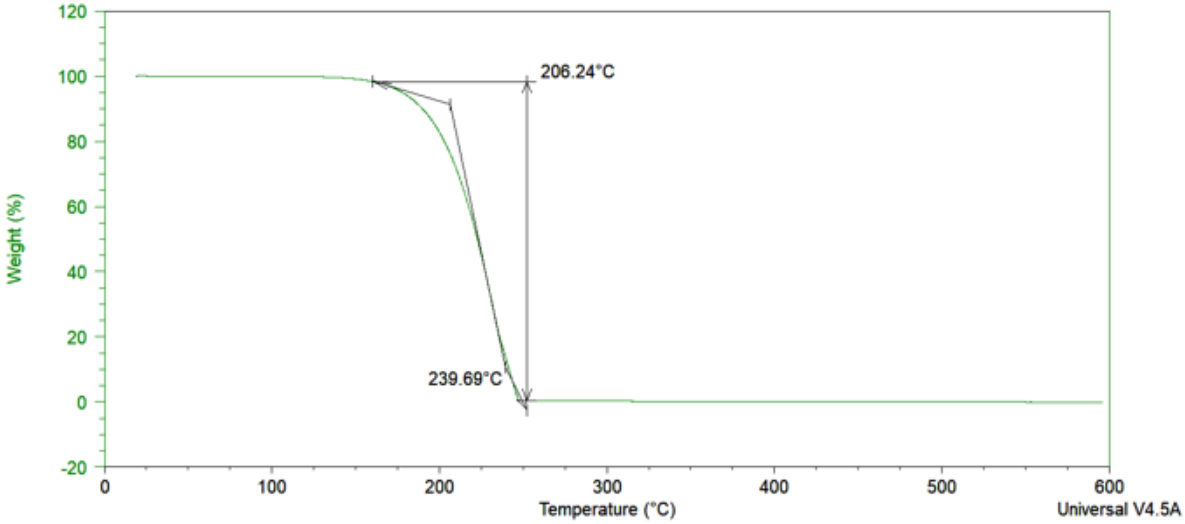

Figure S61. TGA curve of crystals obtained from co-sublimation of **4B** with 40 µL water, with an observed mass loss of 0%.

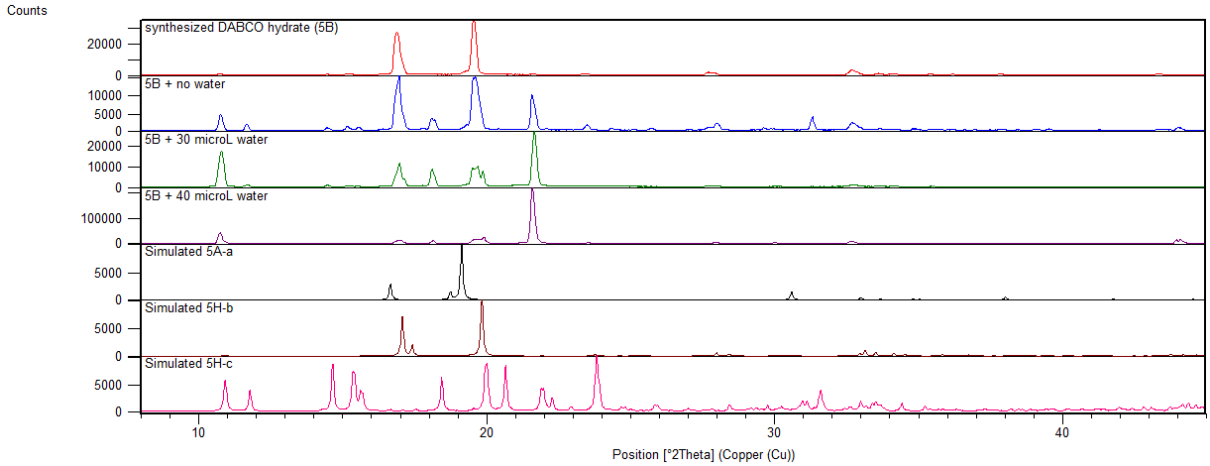

Figure S62. Experimental PXRD pattern of synthesised **5B** (red), **5B** sublimed without water (blue), **5B** sublimed with 30 µL water (green), and **5B** sublimed with 40 µL water (purple), compared to simulated patterns.

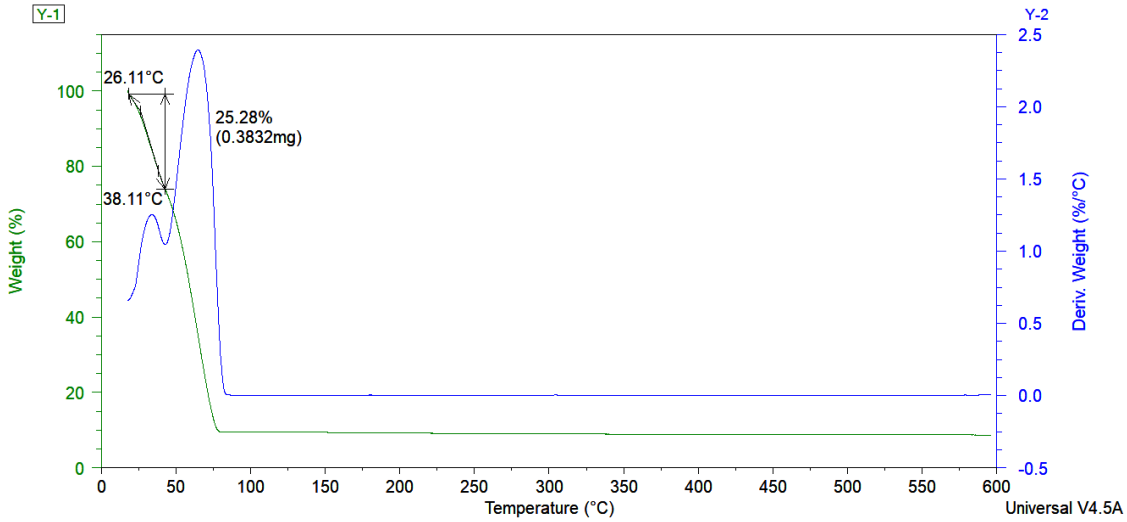

Figure S63. TGA curve of crystals obtained from sublimation of **5B** without water, with an observed mass loss of 25.28%.

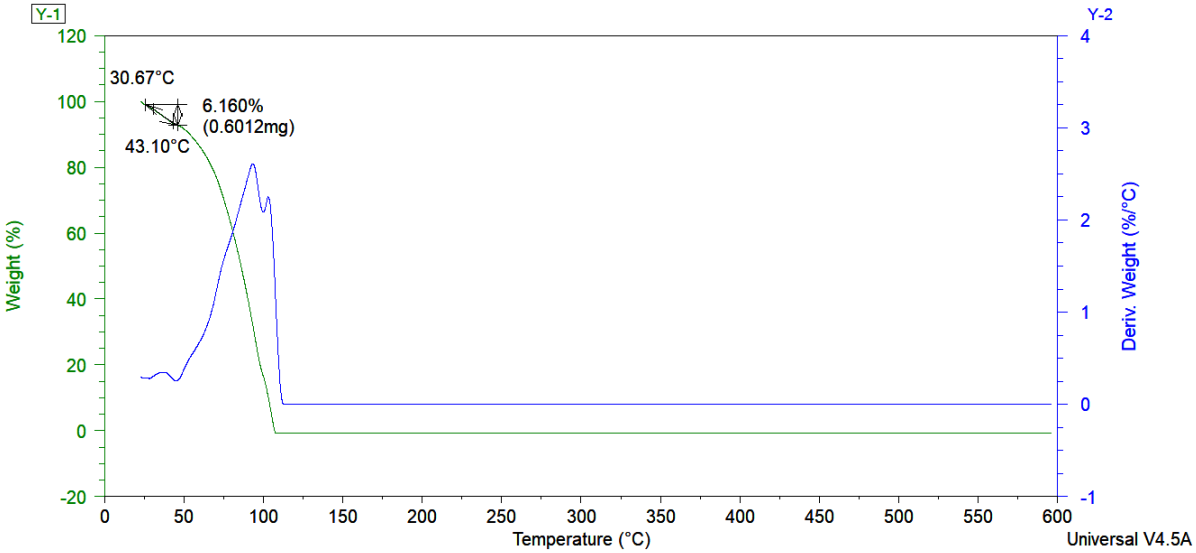

Figure S64. TGA curve of crystals obtained from co-sublimation of **5B** with 30 µL water, with an observed mass loss of 6.16%. Sublimation and decomposition of the sample took place concurrently.

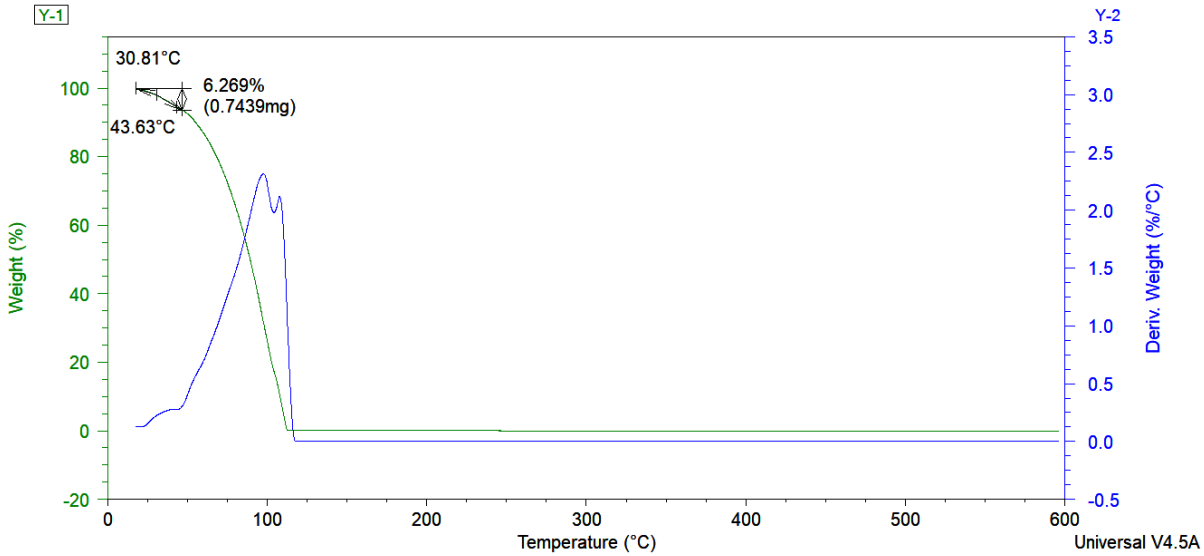

Figure S65. TGA curve of crystals obtained from co-sublimation of **5B** with 40 µL water, with an observed mass loss of 6.27%. Sublimation and decomposition of the sample took place concurrently.

Competition experiments

The co-sublimation results from the competition experiments based on a 1:1 mole-ratio are outlined in Table S8 below, with sublimation conditions and corresponding known crystal forms. PXRD patterns and TGA curves supporting the results obtained from competition experiments follow thereafter.

Table S8. Results obtained from competition experiments with 1:1 mole-ratio co-sublimations of hydrate and anhydrous forms (vacuum pressure of 1.20 mbar).

Hydrate component	Anhydrous component	Sublimation temperature (°C)	Co-sublimation result
1 with mass of 24 mg	**4** with a mass of 37 mg	120	Two bands formed. Top band: **1H-a**[3] (Figure S66) 28.87% water content (Figure S67) Bottom band: **4A-a**[11], **4A-b**[11], **4H- a**[12] (Figure S68) 0.3131% water content (Figure S69)
1 with mass of 24 mg	**5** with mass of 21 mg	120	Two bands formed. Top band: PXRD matches synthesised **5B** (Figure S70) 30.73% water content (Figure S71) Bottom band: PXRD matches synthesised **5B** (Figure S70) 27.29% water content (Figure S72)
2B with mass of 58 mg	**5** with mass of 46 mg	110	Two bands formed. Top band: PXRD matches synthesised **5B** (Figure S73) 14.50% water content (Figure S74) Bottom band: PXRD matches sublimed **2** (Figure S73) 0% water content (Figure S75)

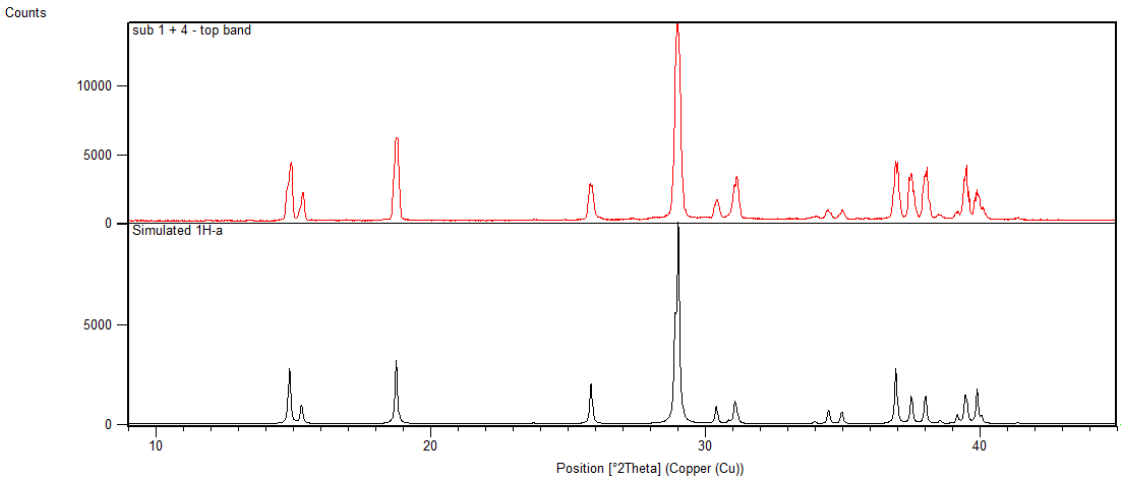

Figure S66. Experimental PXRD pattern of top band of crystals obtained from the 1:1 mole ratio co-sublimation of **1** and **4** in Schlenk tube at 120 °C (red), compared to simulated PXRD pattern of **1H-a**.

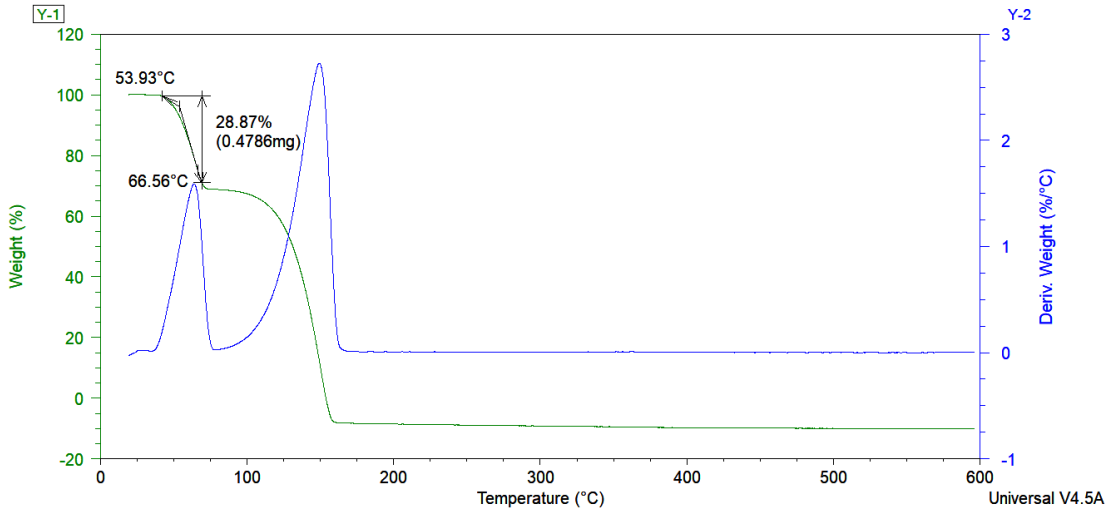

Figure S67. TGA curve of crystals obtained from the 1:1 mole-ratio co-sublimation of **1** and **4** (top band) in Schlenk tube at 120 °C, with mass loss of 28.87%.

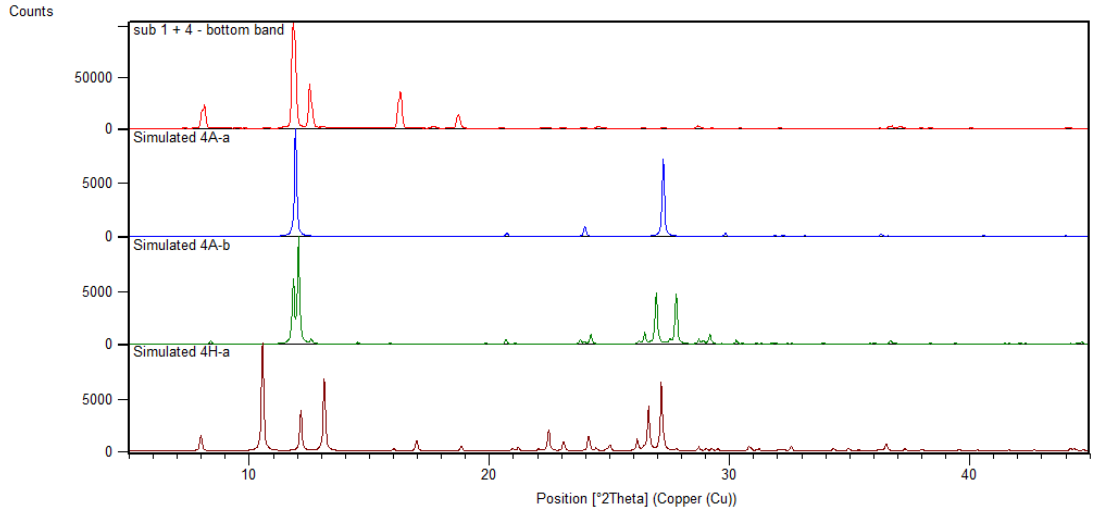

Figure S68. Experimental PXRD pattern of bottom band of crystals obtained from the 1:1 mole ratio co-sublimation of **1** and **4** in Schlenk tube at 120 °C (red), compared to simulated PXRD patterns.

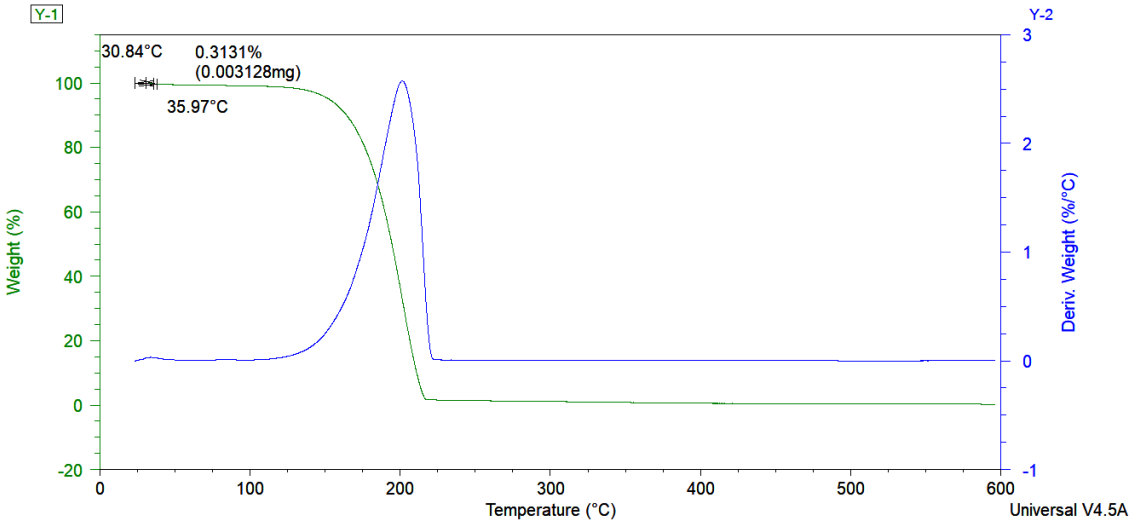

Figure S69. TGA curve of crystals obtained from the 1:1 mole-ratio co-sublimation of **1** and **4** (bottom band) in Schlenk tube at 120 °C, with mass loss of 0.3131%.

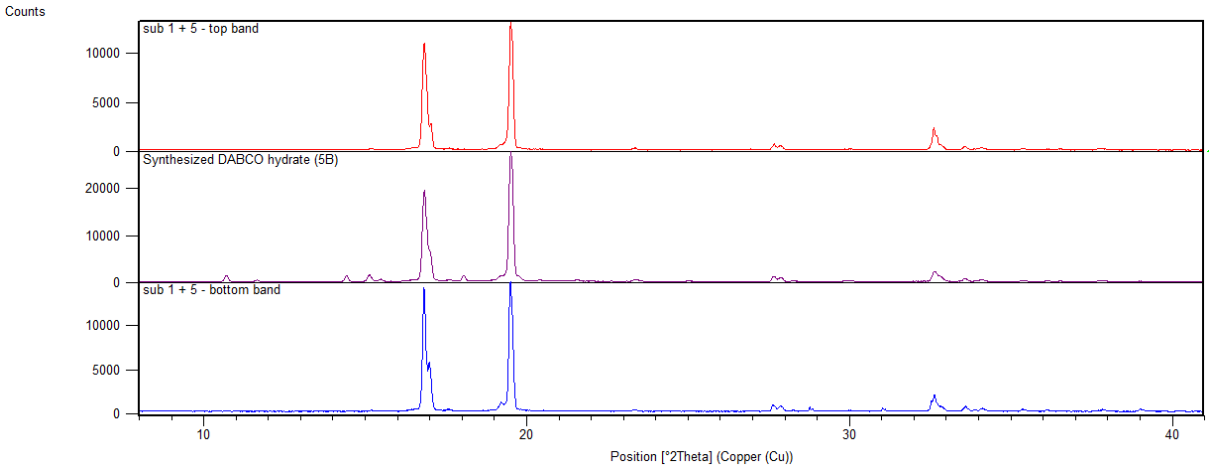

Figure S70. Experimental PXRD pattern of crystals obtained from the 1:1 mole ratio co-sublimation of **1** and **5** in Schlenk tube at 120 °C - top band (red), bottom band (blue), compared to synthesised **5B** PXRD pattern (purple).

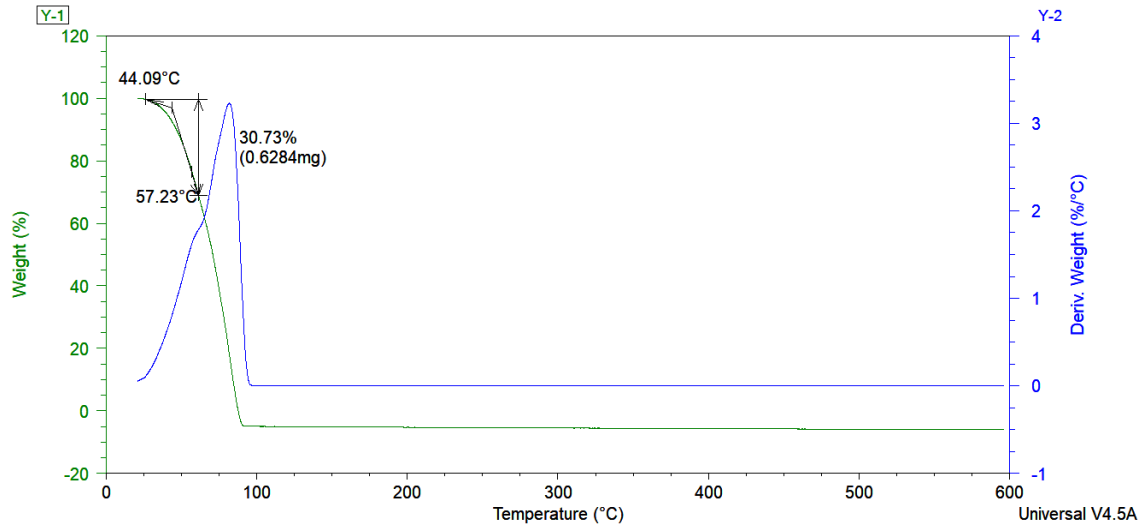

Figure S71. TGA curve of crystals obtained from the 1:1 mole-ratio co-sublimation of **1** and **5** (top band) in Schlenk tube at 120 °C, with mass loss of 30.73%.

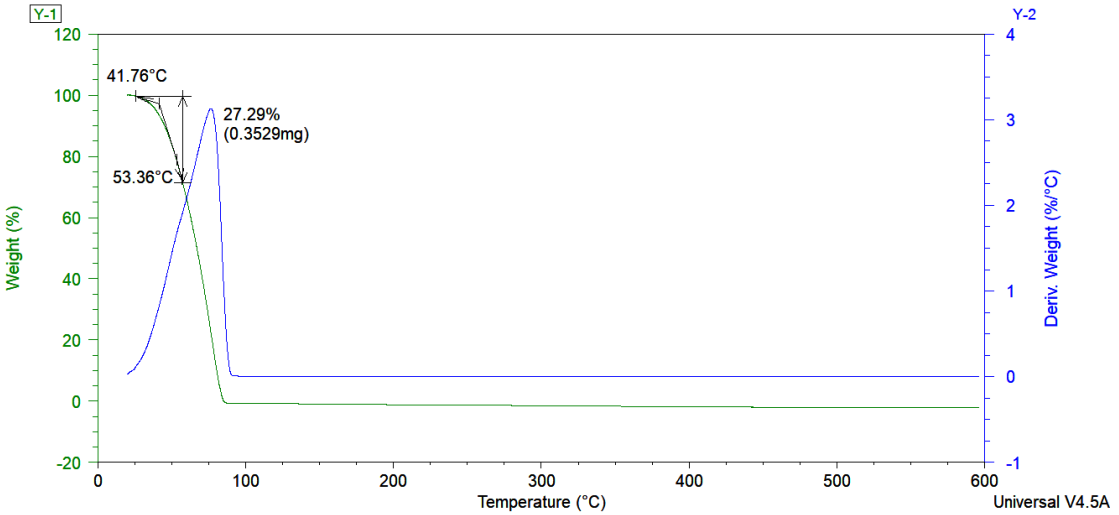

Figure S72. TGA curve of crystals obtained from the 1:1 mole-ratio co-sublimation of **1** and **5** (bottom band) in Schlenk tube at 120 °C, with mass loss of 27.29%.

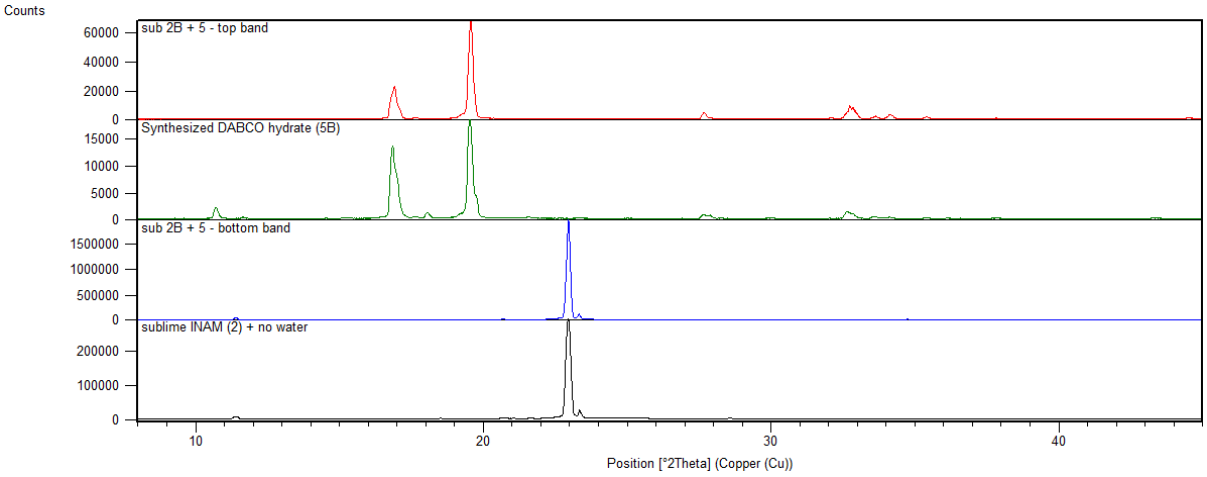

Figure S73. Experimental PXRD pattern of crystals obtained from the 1:1 mole ratio co-sublimation of **2B** and **5** in Schlenk tube at 110℃ - top band (red), bottom band (blue), compared to synthesised **5B** PXRD pattern (green) and PXRD pattern of crystals obtained from sublimation of anhydrous **2** (black).

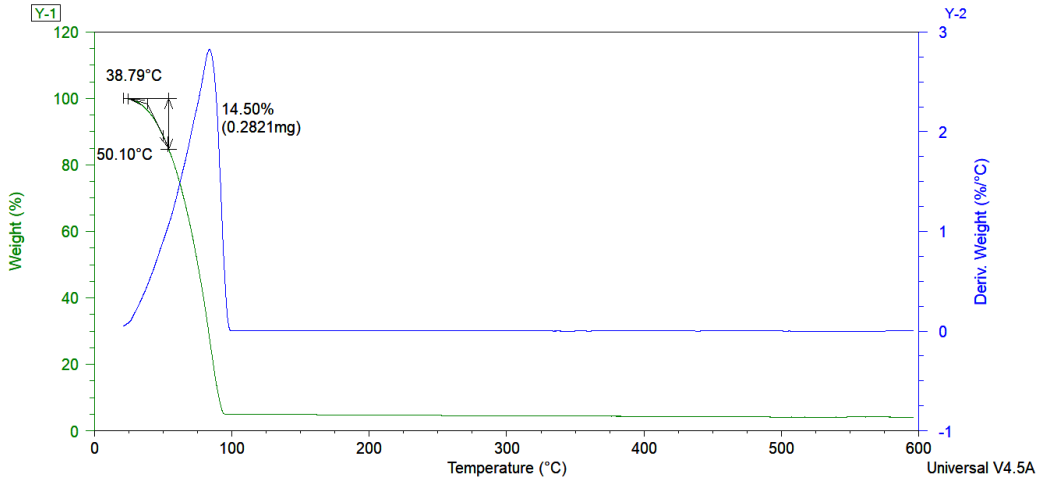

Figure S74. TGA curve of crystals obtained from the 1:1 mole-ratio co-sublimation of **2B** and **5** (top band) in Schlenk tube at 110 °C, with mass loss of 14.50%.

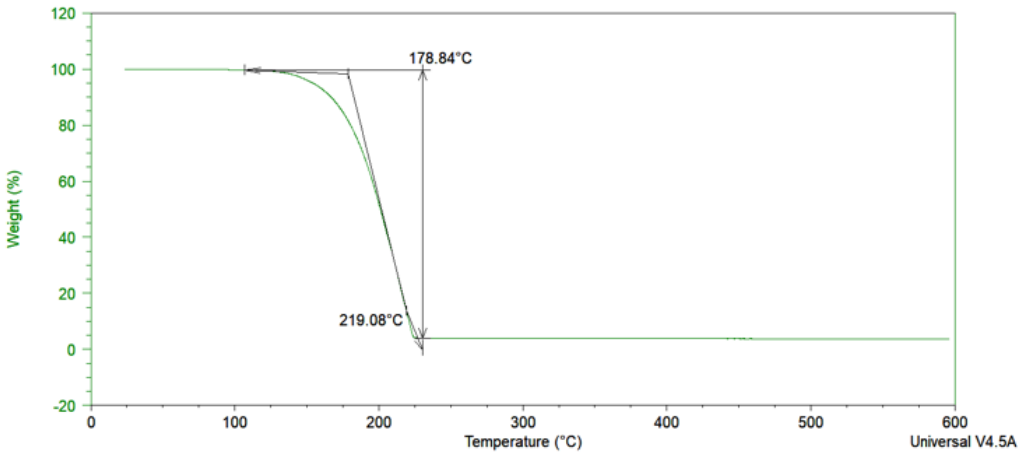

Figure S75. TGA curve of crystals obtained from the 1:1 mole-ratio co-sublimation of **2B** and **5** (bottom band) in Schlenk tube at 110 °C, withmass loss of 0%.

Single-Crystal X-ray Diffraction (SCXRD)

Single-crystal X-ray diffraction (SCXRD) was carried out using a Bruker Duo diffractometer equipped with a CCD area detector, an Incoatec IμS microsource (MoKα, λ = 0.71073 Å) which is coupled with a monochromator assisted with multilayer optics. Data collections were carried out at either room temperature or 100 K, and the temperature was controlled with the aid of an Oxford Cryosystems Cryostat, 700 Series Cryostream Plus. Data collection and reduction were done using the Bruker software package SAINT[16], which operates through the Apex3[16] software. SCXRD was only carried out on a select number of samples where PXRD was found to be inconclusive. Data for unit cell determinations are given in Table S9 below.

Table S9. Single-crystal data unit cell determinations for selected crystals.

Material analysed	**Data-collection temperature (°C)**	**Crystals obtained**	**Unit cell parameters**	**Corresponding known crystalline form**
1 sublimed (no water)	Room temperature	White, needle-like crystals	a = 5.20 Å Å, b = 5.88 Å, c = 5.34 Å, α = 90.00°, β = 115.96°, γ = 90.00°. V = 147 Å^3, Monoclinic P	**1A-b**[2]
2 sublimed (no water)	Room temperature	White, needle-like crystals	a = 10.11 Å, b = 5.77 Å, c = 10.27 Å, α = 90.00°, β = 97.32°, γ = 90.00°. V = 594 Å^3, Monoclinic P	**2A-a**[4]
2B sublimed with 30 μL water	Room temperature	Block-like white grains + small needle-like crystals	a = 9.83 Å, b = 7.91 Å, c = 15.67 Å, α = 90.00°, β = 105.46°, γ = 90.00°. V = 1175 Å^3, Monoclinic P	**2A-b**[4]
3 (as purchased)	100 K	White, long plate-looking crystals	a = 3.77 Å, b = 8.50 Å, c = 24.32 Å, α = 90.00°, β = 90.00°, γ = 90.00°. V = 778 Å^3, Orthorhombic P	**3A-a**[7]
1A sublimed (no water)	Room temperature	White, block-like crystals	a = 6.11 Å, b = 6.57 Å, c = 7.89 Å, α = 90.00°, β = 90.00°, γ = 90.00°. V = 317 Å^3, Orthorhombic P	**1A-b**[2]
		White, needle-like crystals	a = 5.34 Å, b = 6.03 Å, c = 5.44 Å, α = 90.00°, β = 115.83°, γ = 90.00°. V = 158 Å^3, Monoclinic P	**1A-b**[2]

UNI Intermolecular potentials

UNI intermolecular potentials[17] were calculated through Mercury.[18]

The most dominant interaction in the OA dihydrate (**1H-a**)[3] crystal structure is between OA and a water molecule, with an interaction energy of -20.5 kJ/mol. The interaction between two OA molecules is weaker, with an energy of -11.6 kJ/mol (Figure S76).

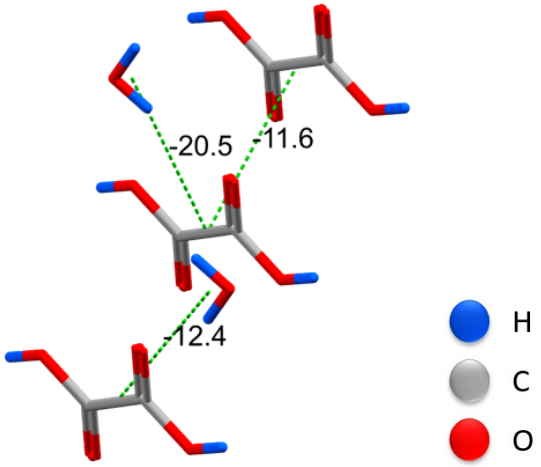

Figure S76. Crystal packing of OA dihydrate (**1H-a**)[3] with calculated interaction energies.

In the INAM monohydrate (**2H-a**)[6] crystal structure, the most dominant interaction is between two INAM molecules with an interaction energy of -30.5 kJ/mol. The interaction with water molecules is much weaker (Figure S77).

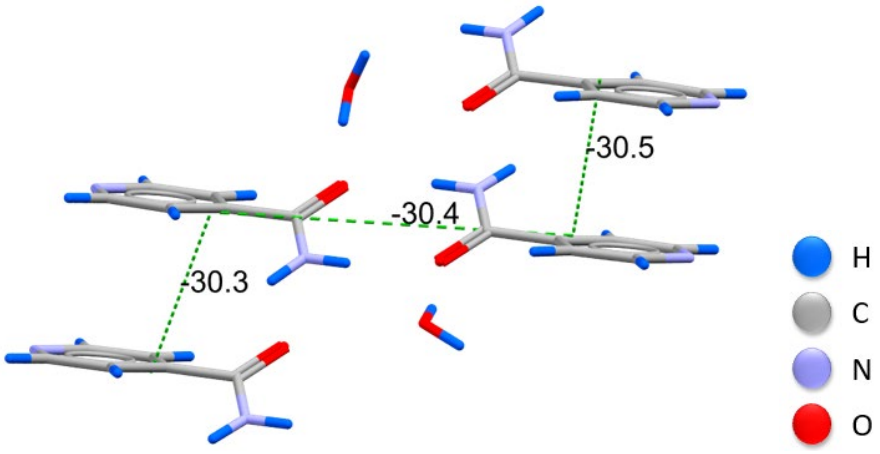

Figure S77. Crystal packing of INAM monohydrate (**2H-a**)[6] with calculated interaction energies.

In the INAM monohydrate (**2H-b**)[6] crystal structure, the most dominant interaction is between two INAM molecules with an interaction energy of -33.2 kJ/mol. The interaction with water molecules is weak (Figure S78).

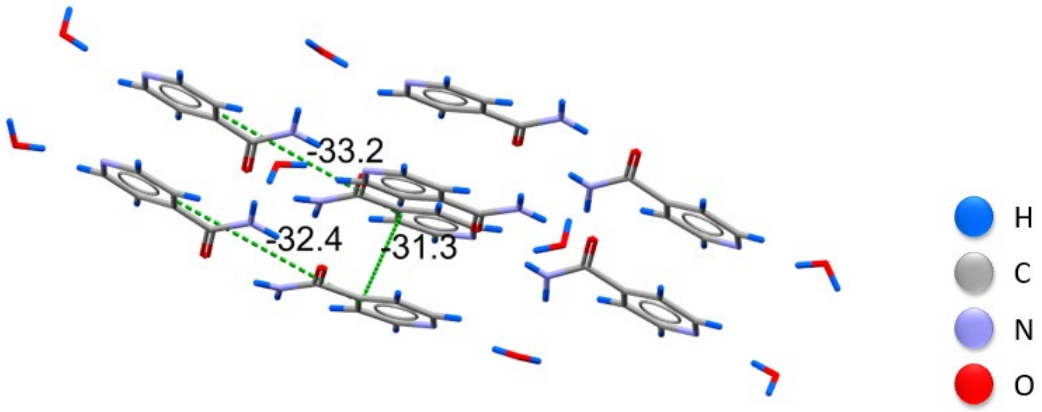

Figure S78. Crystal packing of INAM monohydrate (**2H-b**)[6] with calculated interaction energies.

The most dominant interaction in the crystal structure of THE monohydrate (**3H-a**)[10] is between two THE molecules with an interaction energy of -49.4 kJ/mol. The interaction between THE and water molecules is weaker with an energy of -23.5 kJ/mol (Figure S79).

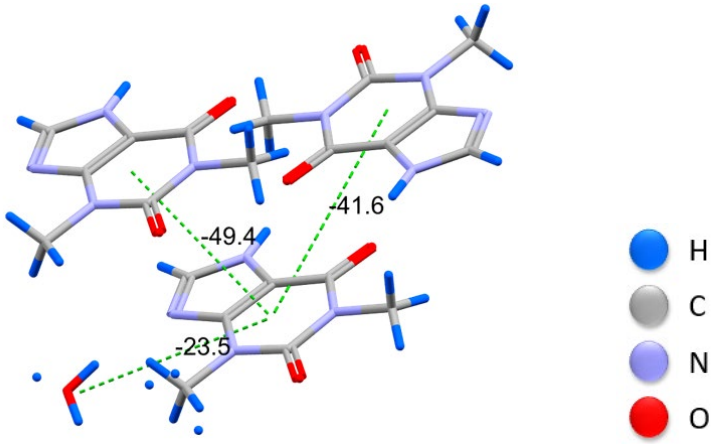

Figure S79. Crystal packing of THE monohydrate (**3H-a**)[10] with calculated interaction energies.

The most dominant interaction in the CAF monohydrate (**4H-a**)[12] crystal structure is between two CAF molecules with an interaction energy of -62.9 kJ/mol. The interaction with water molecules is weaker (Figure S80).

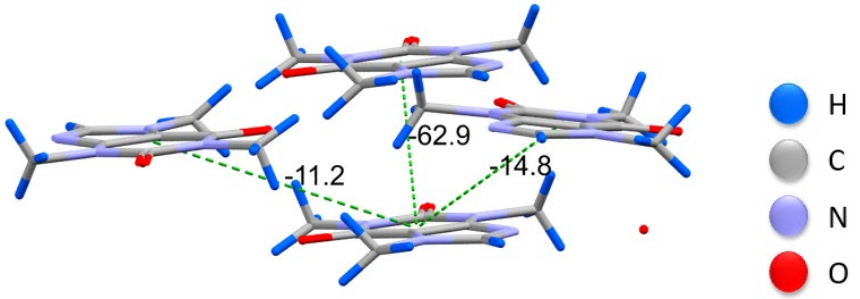

Figure S80. Crystal packing of CAF monohydrate (**4H-a**)[12] with calculated interaction energies.

In the DABCO monohydrate I (**5H-a**)[14] crystal structure, the most dominant interaction is between DABCO and water, with an interaction energy of -24.2 kJ/mol. The interaction between two DABCO molecules is weaker (Figure S81).

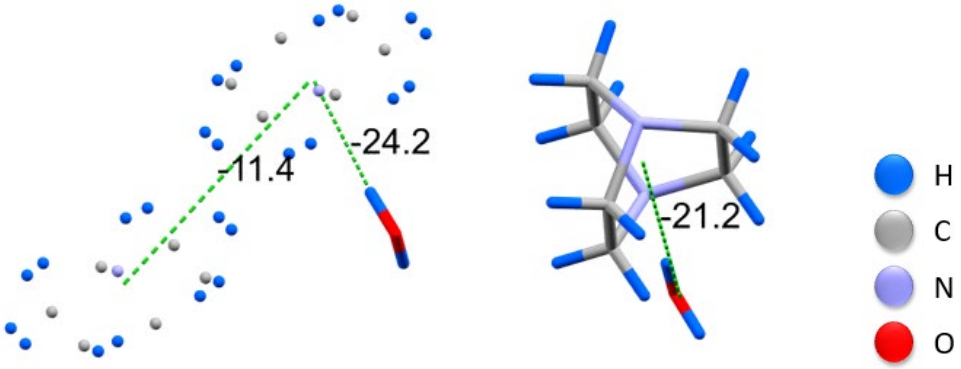

Figure S81. Crystal packing of DABCO monohydrate I (**5H-a**)[14] with calculated interaction energies.

The most dominant interaction in the DABCO monohydrate II (**5H-b**)[15] crystal structure is between DABCO and water, with an interaction energy of -22.3 kJ/mol. The interaction between two DABCO molecules is weaker (Figure S82).

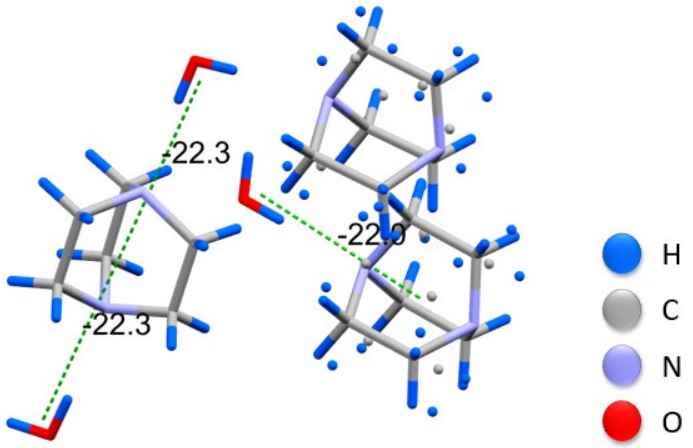

Figure S82. Crystal packing of DABCO monohydrate II (**5H-b**)[15] with calculated interaction energies.

In the DABCO hexahydrate (**5H-c**)[14] crystal structure, the most dominant interaction is between DABCO and water, with an interaction energy of -24.9 kJ/mol. The interaction between two DABCO molecules is weaker (Figure S83).

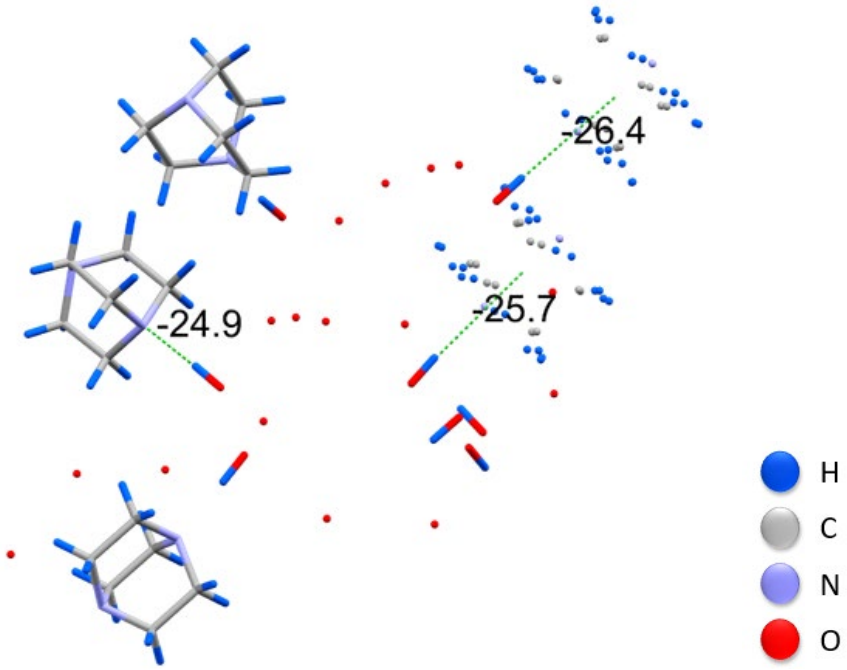

Figure S83. Crystal packing of DABCO hexahydrate (**5H-c**)[14] with calculated interaction energies.

References

1. V. R. Thalladi, M. Nusse, R. Boese, *J. Am. Chem. Soc.*, 2000, **122**, 9227-9236.
2. S. Bhattacharya, V. G. Saraswatula, B. K. Saha, *Cryst. Growth Des.*, 2013, **13**, 3651-3656.
3. R. G. Delaplane, J. A. Ibers, *Acta Cryst.*, 1969, B**25**, 2423-2437.
4. C. B. Aakeröy, A. M. Beatty, B. A. Helfrich, M. Nieuwenhyzen, *Cryst. Growth Des.,* 2003, **2**,159-165.
5. K. S. Eccles, R. E. Deasy, L. Fábián, D. E. Braun, A. R. Maguire, S. E. Lawrence, *CrystEngComm,* 2011, **13**, 6923-6925.
6. N. B. Báthori, A. Lemmerer, G. A. Venter, S. A. Bourne, M. R. Caira, *Cryst. Growth Des.,* 2011, **11**, 75-87.
7. Y. Ebisuzaki, P. D. Boyle, J. A. Smith, *Acta Cryst.*, 1997, C**53**, 777-779.
8. S. Zhang, A. Fischer, *Acta Cryst.*, 2011, E**67**, o3357.
9. K. Fucke, G. J. McIntyre, C. Wilkinson, M. Henry, J. A. K. Howard, J. W. Steed, *Cryst. Growth Des.,* 2012, **12**, 1395-1401.
10. S. Majodina, L. Ndima, O. O. Abosede, E. C. Hosten, C. M. A. Lorentino, H. F. Frota, L. S. Sangenito, M. H. Branquinha, A. L. S. Santos, A. S. Ogunlaja, *CrystEngComm*, 2021, **23**, 335-352.
11. G. D. Enright, V. V. Terskik, D. H. Brouwer, J. A. Ripmeester, *Cryst. Growth Des.*, 2007, **7** (8), 1406-1410.
12. D. J. Sutor, *Acta Cryst.*, 1958, **11**, 453-458.
13. J. L. Sauvajol, *J. Phys. C: Solid State Phys*., 1980, **13**, L927-34.
14. G. Laus, V. Kahlenberg, K. Wurst, T. Lörting, H. Schottenberger, *CrystEngComm*, 2008, **10**, 1638-1644.
15. B. Wicher, M. Gdaniec, *Acta Cryst.*, 2010, C**66**, o270-o273.
16. Bruker APEX3, SAINT and SADABS, Bruker AXS Inc.: Madison, Wisconsin, USA, 2016.
17. A. Gavezotti, *Acc. Chem. Res.*, 1994, **27**, 309–314; A. Gavezzotti and G. Filippini, *J. Phys. Chem.*, 1994, **98**, 4831–4837.
18. C. F. Macrae, I. Sovago, S. J. Cottrell, P. T. A. Galek, P. McCabe, E. Pidcock, M. Platings, G. P. Shields, J. S. Stevens, M. Towler, P. A. Wood, *J. Appl. Cryst.*, 2020, **53**, 226-235.